AN ABSTRACT OF THE THESIS OF

Bryan R. Cobb for the degree of Master of Science in Mechanical Engineering presented on July 8, 2011

Title: Experimental Study of Impulse Turbines and Permanent Magnet Alternators for Pico-hydropower Generation

Abstract Approved:

Kendra V. Sharp

Increasing access to modern forms of energy in developing countries is a crucial component to eliminating extreme poverty around the world. Pico-hydro schemes (less than 5-kW range) can provide environmentally sustainable electricity and mechanical power to rural communities, generally more cost-effectively than diesel/gasoline generators, wind turbines, or solar photovoltaic systems. The use of these types of systems has in the past and will continue in the future to have a large impact on rural, typically impoverished areas, allowing them the means for extended hours of productivity, new types of commerce, improved health care, and other services vital to building an economy.

For this thesis, a laboratory-scale test fixture was constructed to test the operating performance characteristics of impulse turbines and electrical generators.

Tests were carried out on a Pelton turbine, two Turgo turbines, and a permanent magnet alternator (PMA). The effect on turbine efficiency was determined for a number of parameters including: variations in speed ratio, jet misalignment and jet quality.

Under the best conditions, the Turgo turbine efficiency was observed to be over 80% at a speed ratio of about 0.46, which is quite good for pico-hydro-scale turbines. The Pelton turbine was found to be less efficient with a peak of just over 70% at a speed ratio of about 0.43. The lower efficiency can be largely attributed to the rougher surface on the turbine blades. Both turbine types had lower than expected speed ratios which were likely caused by inefficiencies in the turbine. Tests of jet misalignment showed that moving the jet to the inside or outside edge of the buckets caused a drop in efficiency of around 10-20% as well as shifting the optimal speed ratio down 0.03 (6.5%). For the PMA, the generator efficiency peaked at just less than 70%. The data demonstrate the impact of impedance matching on generator efficiency for a PMA.

Currently published literature provides few details specific to Turgo turbines or PMAs despite their suitability for pico-hydro. Nonetheless, Turgo turbines are currently available on the market (at least in the US) and offer a viable option for pico-hydro schemes, particularly in the medium head range. This thesis describes an experimental investigation of impulse turbines, including both Turgo and Pelton turbines, which will be useful for implementation of rural electrification projects. The

results stress the importance of proper system design and installation in order to ensure a successful scheme.

Experimental Study of Impulse Turbines and Permanent Magnet Alternators for Pico-hydropower Generation

by
Bryan R. Cobb

A THESIS

Submitted to

Oregon State University

in partial fulfillment of
the requirements for the
degree of

Master of Science

Presented July 8, 2011
Commencement June 2012

Master of Science thesis of Bryan R. Cobb presented on July 8, 2011.

APPROVED:

Major Professor, representing Mechanical Engineering

Head of the School of Mechanical, Industrial, and Manufacturing Engineering

Dean of the Graduate School

I understand that my thesis will become part of the permanent collection of Oregon State University libraries. My signature below authorizes release of my thesis to any reader upon request.

Bryan R. Cobb, Author

ACKNOWLEDGEMENTS

I would like to acknowledge and thank all those whom have made contributions to my research and the writing of this thesis. The guidance and encouragement from my advisor Dr. Kenda Sharp have been instrumental to my success in this academic endeavor. Thanks also to Caleb Calkins for his assistance in the lab carrying out experiments and my team of editors and proofreaders including my parents, Rachel Yim and Mary VanSteenberghe.

I would also like to express my appreciation to all of my friends, family and colleagues whom have provided support me and much needed distractions from my studies along the way. It has been a pleasure working with everyone in the thermal fluid sciences group at Oregon State University. Thank you to the Finney family (and extended family) for all the support they have provided over the last two years, including many meals and a place to stay on numerous weekends. Also, thank you to my parents for all of their support during this program and in life.

TABLE OF CONTENTS

TABLE OF CONTENTS (Continued)

LIST OF FIGURES

LIST OF FIGURES (Continued)

LIST OF FIGURES (Continued)

LIST OF TABLES

LIST OF APPENDIX FIGURES

NOMENCLATURE

A	area
d	diameter
f	friction factor
g	gravitational acceleration
H	hydraulic head
I	current
K_L	head loss coefficient
l	length
N	rotational speed (rpm)
N_s	specific speed
p	pressure
PCD	pitch-circle diameter
Q	volumetric flow rate
U	tangential turbine speed
v	velocity
V	voltage
W	rate of work, power
x	speed ratio
z	elevation
α	reference angle between water and turbine
β	absolute angle between water and turbine

NOMENCLATURE (Continued)

γ	jet angle
η	efficiency
ρ	density
ω	shaft speed (radians per second)

Subscripts

c	combined
e	effluent
elec	electrical
g	gross
gen	generator
h	hydraulic
i	influent
j	jet
l	loss
n	net
noz	nozzle
s	shaft
t	turbine

Experimental Study of Impulse Turbines and Permanent Magnet Alternators for Pico-hydropower Generation

Chapter 1 – Introduction

Across the globe, 1.4-1.6 billion people have no access to electricity at all while another one billion are dependent on unreliable electrical grids [1]. In addition, as many as three billion people rely on antiquated solid fuel sources for cooking and heating [2]. The United Nations (UN) has underscored the importance of global access to electricity by setting a goal to achieve what it refers to as "universal access to modern energy services" by 2030 [2]. The estimated price tag to meet this goal is $36 billion per year [2]. Since many of those lacking access to modern energy live in rural areas, decentralized, off-grid energy projects will play a vital role in achieving the UN's energy goal by 2030 [3]. Over the last 30 years, pico-hydropower (hydropower facilities generating less than 5 kW) has been proven as a cost-effective, clean, and reliable method of generating electricity and mechanical power for off-grid applications and will play an important role in rural electrification into the foreseeable future.

Access to modern forms of energy can have a tremendous impact on the lives of impoverished people living in developing countries by reducing manual labor, encouraging economic activity, improving health conditions, and reducing the overall cost of energy [2, 4]. The mechanical power produced can be utilized for vital industrial and agricultural processes such as milling grain, running water pumps for irrigation, and powering refrigeration cycles, to name a few applications [3, 5]. The electricity produced can also serve a number of useful purposes, namely home lighting. Electrical lighting can increase the productive hours in the day, thereby allowing more time for education and economic productivity. Kerosene lamps and

candles, common alternatives for lighting when electricity is not available, cost more over time and produce poor quality light [6]. Additionally, electricity can be used to power computers, radios and other equipment essential to schools, medical clinics, and businesses [7]. A 2008 survey in Bhutan found that after a small-scale hydropower system was installed, residents of the village of Sengor needed half as much wood for fuel as before, and furthermore benefitted from an average of 1.5 additional hours of light per day [8].

Pico-hydropower, consisting of small water driven electrical generators producing less than 20-kW of power, has garnered significant attention in the last 30 years for its ability to meet the energy needs of rural communities in developing countries. In Nepal for instance, 1200 pico-hydro schemes have been constructed by Practical Action (formerly ITDG), of which 300 produce electricity [9]. The roughly 900 other installations are used for mechanical power only. Practical Action has also been involved with the construction of another 70 installations in Sri Lanka and 15 in Peru in recent years [9]. In the last decade, pico-hydro has become more prevalent in Sub-Saharan Africa as well, where electrification rates are some of the world's lowest [10]. As of 2003, many as 50 million households worldwide receive electricity from hydropower on mini-grids, with several hundred thousand units installed [4].

A number of advantages set pico-hydropower apart from other electrical generation methods for rural areas. Keeping costs low is often one of the most important considerations for rural electrification projects since the customers typically

have limited funds [3]. Figure 1.1 compares the cost of commonly used power sources in the range of power needed for rural electrification.

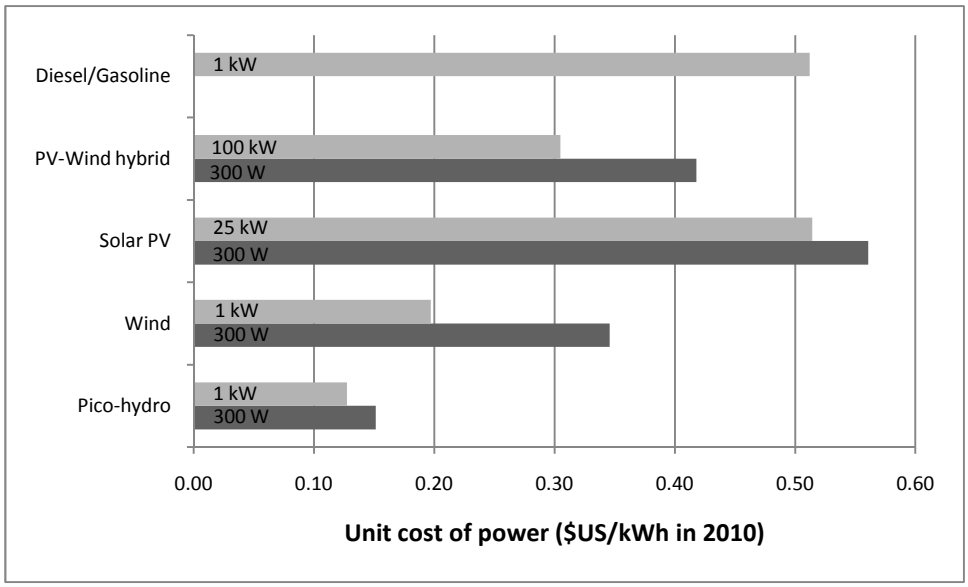

Figure 1.1. Predicted operating cost of off-grid electricity for various sources (data from the World Bank [11]).

Provided the water resources are available, hydro is nearly always the lowest cost power source for the long term operation. Inexpensive standardized equipment that can be manufactured locally and a local labor force for installation help to keep capital costs down while minimal maintenance requirements and no fuel costs keep long term operations affordable [11, 12].

From an environmental stand-point, pico-hydro power has a relatively minor impact on the surrounding ecosystem. Schemes in the pico- size range are typically run-of-the river so they do not share the same ecological drawbacks as larger hydro

plants such as interfering with fish migration patterns and emitting green house gasses [13].

Additionally, water flow in rivers and streams can often be predicted based on weather patterns and seasonal trends [14] which translates into a more reliable form of power. Other renewable energy sources such as wind and solar can vary significantly throughout the day making power production unpredictable. Solar photovoltaic cells cannot be counted on to produce power after the sun goes down, when lighting is most needed, and wind turbines only work when the wind is blowing.

While pico-hydro presents significant advantages over other types of electricity generation, implementation of it can present a challenge and is thus a drawback [13]. Scheme design is heavily dependent on site-specific conditions that must be properly accounted for [15]. Off-the-shelf systems have been designed to reduce the site specific design but this does not completely eliminate the need for technical expertise [16]; in order to ensure long term success of projects, care must be taken in the design process to select the correct parts and install them properly. Additionally, community cooperation is necessary for day-to-day management, though maintenance should not be overly difficult or time consuming.

Funding for rural electrification in developing countries comes from a number of different sources including the United Nations Development Programme, the World Bank, the Asian Development Bank, government agencies, and various non-government organizations (NGOs). The US government agencies involved with pico-

hydro include the Agency for International Development (USAID), the Department of Agriculture (USDA), and the Army Corps of Engineers. As of 2007, the UN contributes about $2.5 billion per year to off-grid electrification projects in developing countries while the World Bank contributes another $500 million [2, 17]. Funds are often provided as interest-free micro loans to communities to cover the capital costs of installation with the loans paid back over time with money raised by electricity rates charged to the users. In addition to providing project funding, the aid organizations involved provide technical expertise for design, planning, installation, and operation of the plants.

1.1 Motivation

Two important concerns for implementing pico-hydropower in developing countries are to ensure that (1) appropriate technology exists and (2) understanding and awareness of such technology exists [13, 16]. Appropriate technology for pico-hydro includes low-cost civil works, locally manufactured and/or standardized components, including turbines and generators, and efficient load management equipment. Proper understanding of pico-hydro technology will improve the likelihood of successful installations. Awareness can be generated by working with organizations on the ground in the countries where rural electrification projects are needed.

One area of appropriate technology for pico-hydro that has lacked adequate attention up to this point is the use of Turgo turbines. While Turgo turbines offer

many of the same advantages of Pelton turbines, such as high efficiency for a broad range of site conditions, they also allow for much higher flow rates of water for the same size turbine because of the flow path through the turbine. This advantage not only means a smaller, less expensive turbine can produce the same amount of power but also that the Turgo turbine can also be useful at lower hydraulic heads than a comparable Pelton. Currently, pumps-as-turbines (PATs) are commonly used for medium head schemes; however Turgo turbines may also be a viable solution.

Unfortunately, at the moment there is little literature specifically addressing the application of Turgo turbines for pico-hydro, rather, emphasis has been placed on Pelton turbines. Obtaining turbine data from manufacturers and distributors in the United States (US) has proven difficult. Energy Systems & Design [18], manufacturer of the Stream Engine, a Turgo turbine-generator set, reported peak turbine efficiencies of approximately 70% and 80% for a Gilkes and their in-house designed Turgo turbines used in their products [19]. More detailed specifications for varying site conditions (different heads, flow rates, jet diameter, etc.) were not available. Other companies such as Nooutage.com do provide data on their website [20] for different head and flow rate conditions; however, efficiencies are reported as water-to-wire efficiency (including nozzle, turbine, and generator efficiency).

Additionally, a number of case studies of do-it-yourself (DIY) installations are available on the Home Power Systems website [21]. For most schemes, head, flow

rate, and electrical power are provided and water-to-wire efficiency can be calculated. A summary of a selection of the case studies is presented in Table 1.1.

Table 1.1. Summary of select DIY pico-hydro case studies (data from Home Power Systems [21])

Scheme	Head (ft)	Flow Rate (gpm)	Hydraulic Power (W)	Electrical Power (W)	Water-to-wire efficiency
1	157.5	110	3258	1120	0.344
2	80	250	3761	780	0.207
3	90	150	2539	1500	0.591
4	110	130	2689	240	0.089
5	200	150	5641	1800	0.319
6	150	110	3103	216	0.070

Water-to-wire efficiency is quite low on most of the installations, ranging from 7% up to 59%. The expected efficiency should be closer to 50-60%. Without any data on component efficiencies, it is difficult to determine why the overall efficiency is so low.

Data on Turgo turbine performance is not readily available on the turbines in use today making it difficult to design systems with reasonable operating efficiencies. A study that demonstrates how parameters such as speed ratio (ratio of tangential turbine velocity and jet velocity), system design, and installation impact turbine efficiency would improve Turgo turbine implementation. Installers would have a

better idea of what the expected system efficiency should be as well as better understand the operating conditions that will produce the best efficiency.

A second area of interest is the use of permanent magnet alternators (PMA) as electrical generators. Induction generators have been the preferred generator in the past because of their availability and reliability [13]. PMAs, which require no brushes, can be just as reliable as induction generators. The permanent magnet rotor means a magnetic field can be generated in the rotor without the use of an external power supply resulting in a more efficient generator as compared to conventional alternators and induction generators. Practical information on the use of PMAs in pico-hydro such as the impact of input conditions on operating efficiency is not currently available.

1.2 Objectives

The goals of this research are to construct a laboratory scale test fixture for use in education and research related to pico-hydropower and to experimentally validate the following hypotheses: 1) Turgo turbine efficiency depends on speed ratio similar to the way Pelton turbines do, 2) jet misalignment must be minimized in order to maximize energy transfer from the water jet to an impulse turbine, 3) a high quality jet, characterized by minimal secondary flow structures, is necessary to maximize energy transfer from the water jet to the impulse turbine, 4) turbine efficiency for a particular flow rate and head may be scaled to another flow and head over a certain range, 5) generator efficiency for a permanent magnet alternator depends on both shaft

speed and power output, and 6) a turbine and permanent magnet alternator must be properly matched based on operating speed for the desired power output to achieve optimal combined turbine-generator efficiency. The study presented in this thesis will investigate several potential pitfalls of poorly managed pico-hydro installations. Particular emphasis will be given to the use of Turgo turbines; however, Pelton turbines will be addressed as well. The results will indicate the most important conditions for consideration in order to ensure an efficient final product.

Chapter 2 – Pico-hydro System & Components

2.1 Hydropower Classifications

Hydropower classification on the basis of size varies from one reference to another [16, 22-25]; however, the distinctions made are often made arbitrarily [23]. A widely accepted classification system for hydropower is presented in Table 2.1.

Table 2.1. Classification of hydropower (adapted from Sopian [22]).

Power	Class
>10 MW	Large
<10 MW	Small
<1 MW	Mini
<100 kW	Micro
<5 kW	Pico

For the purposes of this study, the definitions of hydropower classifications given in Table # will be used, with the pico range being the focus. Here, a distinction between pico and micro-hydro, in accordance with the definitions given by Williams [26] has been made because schemes in the less than 5 kW range tend to be cost effective only if standardized equipment can be implemented. Standardized equipment, or modular equipment as it is sometimes referred to as, can minimize site-specific design without sacrificing too much operating efficiency. In another study by Alexander and Giddens [16], micro-hydro was distinguished from mini-hydro and classified as less than 20 kW, using similar reasoning, while the term pico-hydro was not used. This range, where minimal site-specific work is necessary for maintaining reasonable costs is the focus for this thesis. Making a determination as to whether standardized equipment should be used for hydropower application below 20 or 5 kW was outside the scope of

this thesis. The lesser value, 5 kW will be used throughout this work since it appears to be more widely used though the findings herein may also be applicable above the pico-hydro range.

2.2 Typical Scheme

A pico-hydro scheme typically consists of a weir that diverts water from the river to a forebay. The forebay, which is generally open to the atmosphere, acts as a settling pond to reduce the sediment in the water. From the forebay, the water is carried by the penstock to the power house, where the turbine and generator are located. Pressure builds in the water as it descends in elevation through the penstock to the power house where it is forced through a nozzle that accelerates the water and forms a high-velocity free jet. Energy is transferred from the water to the turbine as the jet impinges on the turbine blades causing the turbine and shaft to rotate. The turbine is coupled with an electrical generator that produces electricity which can then be distributed to electrical loads (i.e. the users) by transmission lines. Downstream of the turbine, the water can be returned to the same river by the tailrace. This type of set up is referred to as “run-of-the-river” scheme because no dam is required to obstruct the natural flow of the river. Figure 2.1 provides an illustration of a typical scheme.

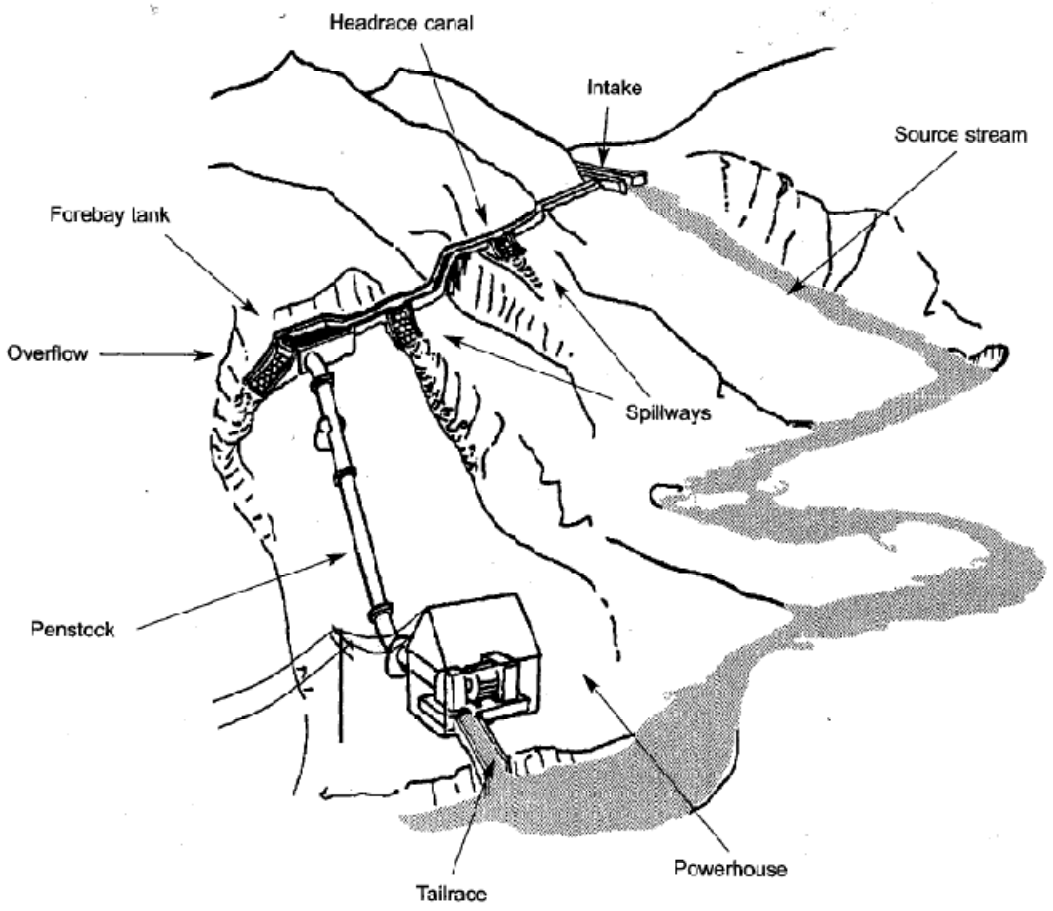

Fig. 2.1. Typical pico-hydropower scheme (figure used with permission from Practical Action Publishing [24]).

2.3 Current Technology

2.3.1 Turbines

Water turbines used for pico-hydro are typically broken down into two classifications: reaction and impulse. Reaction turbines rely on a pressure drop in the water across the turbine to transfer energy to the shaft while impulse turbines transfer the moment of a high velocity water jet to the turbine [24]. Both types are commonly

used for small scale hydropower with the selection depending on the head and flow rate conditions of the site. Head is often broken down into several classifications, low, medium, and high, defined as less than 10 m, 10-50 m, and greater than 50 m [23]. Table 2.2 lists the types of turbines typically used for a given head condition.

Table 2.2. Classification of turbines used for pico-hydro based on hydraulic head and type (adapted from Paish [23]).

Turbine Type	Low (<10 m)	Medium (10-50 m)	High (>50 m)
Impulse	Crossflow	Crossflow Turgo Pelton	Turgo Pelton
Reaction	Francis Propeller Kaplan	Francis	

Reaction turbines are further split into Francis, propeller and Kaplan turbines [23] pictured in Figs. 2.2 and 2.3. Using centrifugal pumps-as-turbines, or PAT, [26] has also been suggested; those operate as reaction turbines. Typically, reaction turbines operate under low and sometimes medium head conditions (<10 and 10-50 m respectively) and high flow rates [23]. Reaction turbines can handle very high flow rates due to the turbine geometry and flow of the water through the blades making them the preferred turbines for low-head high-flow applications. The main disadvantages are that efficiency is reduced dramatically when head and flow rate are not near design conditions and they generally require complicated (expensive) turbine housings. Pictures of various reaction turbines are shown in Figs. 2.2-2.4.

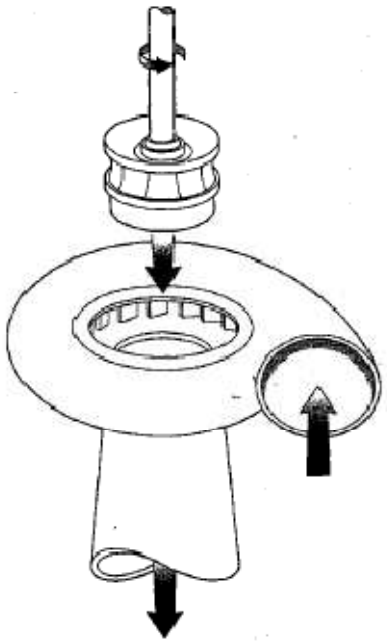

Fig. 2.2. Francis turbine (used with permission from Practical Action Publishing[24]).

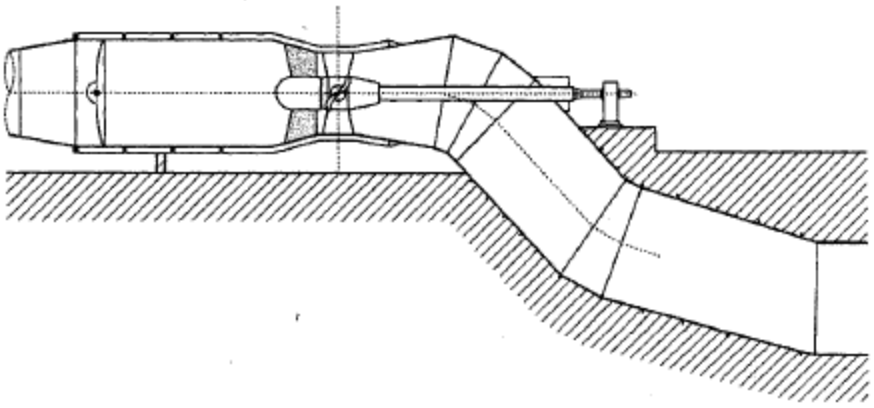

Fig. 2.3. Propeller of Kaplan turbine (used with permission from Practical Action Publishing [24]).

Impulse turbines, which will be the focus of this study, consist of Pelton, Turgo and cross-flow turbines.

A Pelton turbine, shown in Fig. 2.4, is usually used for high head and low flow rate conditions [13]. Pelton turbines offer high operating efficiency over a wide range of flow conditions, are widely available, and are fairly inexpensive to manufacture making them a common choice for high head applications. Due to the cup design however, higher flow rates tend to lead to interference between water entering and with the water exiting the bucket resulting in poor efficiency at high flow rates. Empirical data suggests that turbine efficiency begins to drop when nozzle diameter exceeds approximately 11% of PCD [24]. Above this limit, flow interactions inside the turbine cups become more significant and reduce turbine efficiency. Though turbine efficiency drops when nozzle diameter exceeds 11% of PCD, it may still be advantageous to use a larger nozzle, provided the power increase resulting from the higher flow rate offsets the power lost to the reduction in efficiency [13]. Larger flow rates can also be achieved by adding additional jets. For pico-hydro, up to 4 jets are commonly used on vertical axis and up to 2 jets on horizontal axis installations [24]. Turbines ranging in pitch-circle-diameter (PCD) from 100 to 400 mm can cover most applications up to 100 kW with heads up to 200 m, where PCD is the diameter of the turbine measured to where the jet strikes the turbine.

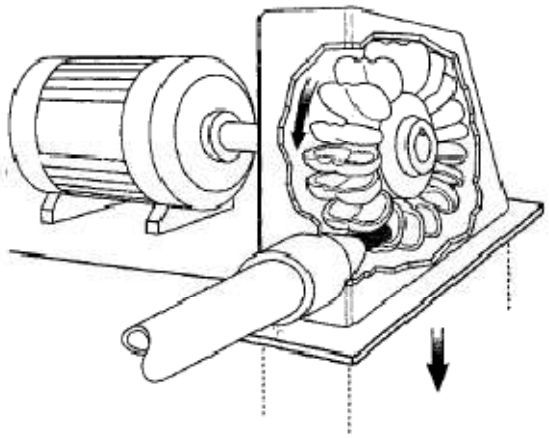

Fig. 2.4. Pelton turbine (used with permission from Practical Action Publishing [24]).

A Turgo turbine, as shown in Fig. 2.5, like the Pelton turbine, is also useful for high head and low flow rate conditions. Additionally, since water passes *through* the Turgo turbine (i.e. in one side and out the other) higher flow rates can be handled. With higher flow rates, Turgo turbines can operate effectively at lower head conditions than the Pelton turbines but are still classified as medium to high head turbines.

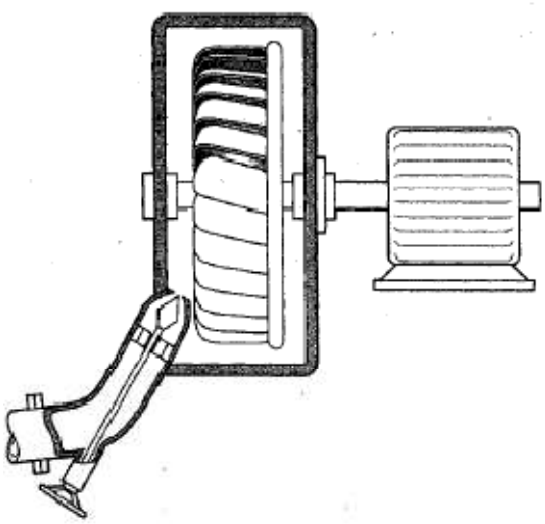

Fig. 2.5. Turgo turbine (used with permission from Practical Action Publishing [24]).

A cross-flow turbine, pictured in Fig. 2.6, is used for low head and high flow rate conditions. A rectangular nozzle directs the water flow across the width of the turbine. Most of the water's kinetic energy is transferred to the runner as it enters with a little more imparted upon exiting the turbine. They typically have lower peak operating efficiencies compared to other turbines but can operate near peak efficiency for a wide range of flow conditions, unlike other low head turbines such as propeller and Francis turbines. Figure 2.7 shows turbine efficiency as a function of the proportion of design flow for different turbine types. A well designed (fully engineered) cross-flow turbine can achieve an efficiency as high as 85%; whereas, locally-made versions tend to fall in the 60-75% efficiency range [14]. Cross-flow turbines also tend to be easier to manufacture than other low head turbines because (1) they do not require complicated turbine cases and (2) the turbine geometry is simpler.

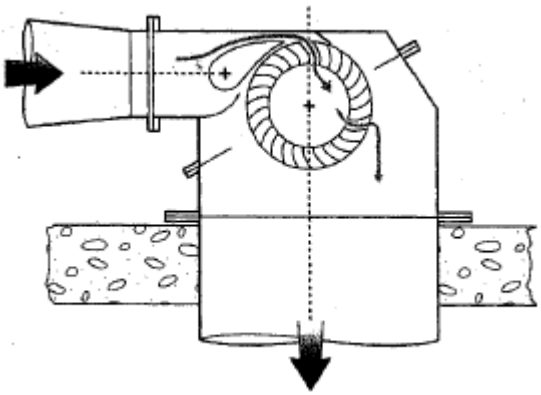

Fig. 2.6. Cross flow turbine (used with permission from Practical Action Publishing [24]).

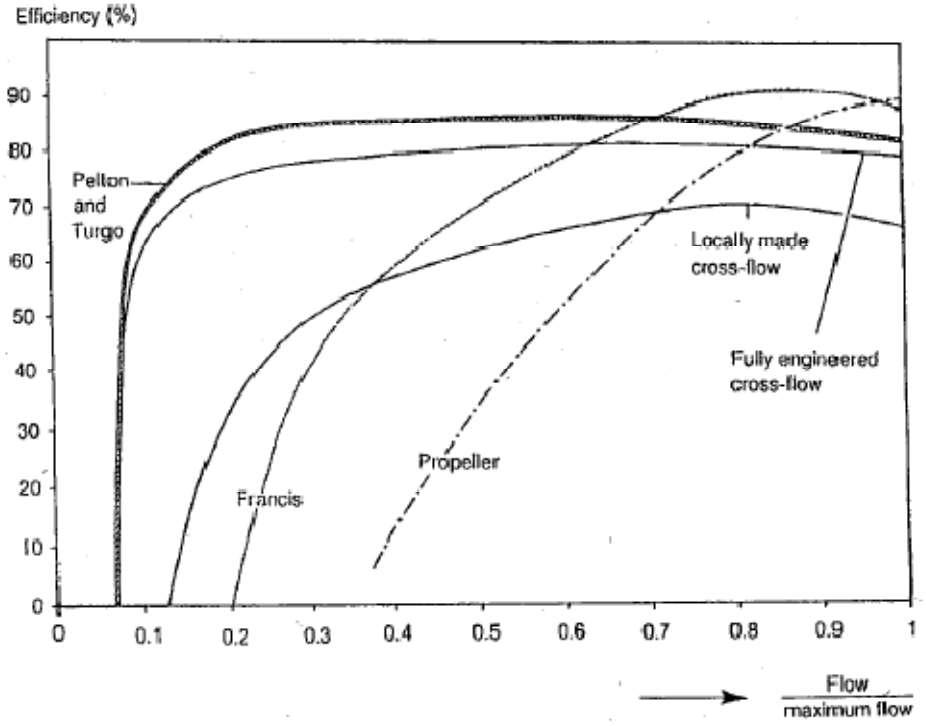

Figure 2.7: Turbine efficiency vs. proportion of design flow for various turbine types (used with permission from Practical Action Publishing [14]).

For medium-head applications, a Turgo turbine, Pelton turbine or a pump-as-turbine (PAT) will most likely be the best choice. The selection among these three

turbine types will depend on availability of equipment, costs, and variability of site conditions, among others. PATs offer a coupled turbine-generator set that has a peak efficiency comparable to Pelton and Turgo turbine systems. The downside of PATs is that they must be sized for a particular flow rate to operate near its best efficiency point [26]. Since pumps are available in many sizes at low costs, they are often used. Pelton turbine systems for medium head may require more than one jet and/or a larger (more expensive) turbine connected to the generator by a pulley in order to accommodate enough flow to produce the desired amount of power [24]. Despite these modifications that add to the complexity and cost of the system, Pelton turbines can operate near their peak efficiency point even with variations in flow rate. As figure 2.7 shows, peak efficiency varies only a few percent from about 20% of rated flow up to 100%. Additionally, effective Pelton turbines can be constructed locally at low costs making them available nearly everywhere. Turgo turbines can handle much higher flow rates than Pelton turbines and can still maintain good turbine efficiency with variations in flow rate. Like Pelton turbines, Turgo turbines designs exist that can be easily manufactured locally in developing countries to help keep capital costs low. Each of the three turbine types is suitable for pico-hydro in the medium head regime; however, the Turgo turbine is the most versatile. The Turgo turbine could be effectively used for the majority of medium-head pico-hydro installations. One potential reason Turgo turbines have been overlooked in the past is that previous designs were cast as a single piece [27], making local manufacture with basic

techniques impractical. The Turgo turbine design tested in this study however, can be built using manufacturing techniques available in developing counties.

In the United States and Canada, various turbine-generator sets are available from retailers. Pico-hydro equipment vendors often provide charts displaying the applicable ranges of head and flow rate for a particular turbine-generator set as shown in Fig 2.8.

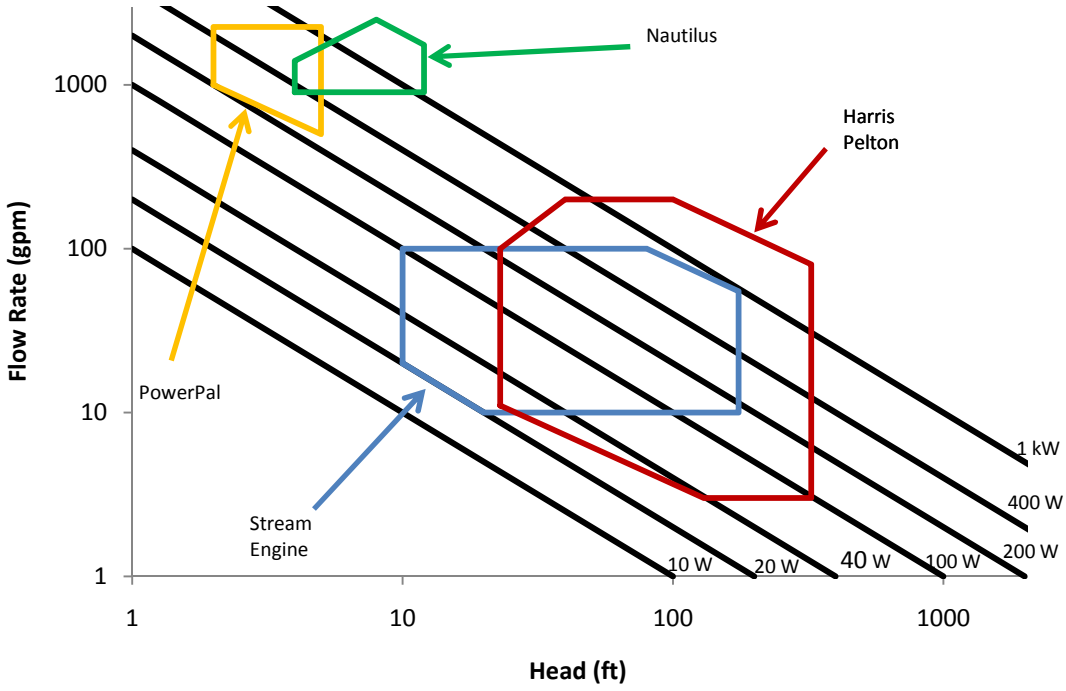

Fig. 2.8. Log-log plot of head vs. flow rate showing applicable operating ranges for various turbine-generator sets available in North America (adapted from ABS Alaskan Hydro Power Design Booklet [28]).

The chart in Fig. 2.8 shows where each type of system is most effective at producing electricity and can be helpful in turbine selection. A water-to-wire efficiency

(combines nozzle, turbine, and generator efficiency) of approximately 53% is assumed for each of the turbine-generator sets shown in Fig. 2.8. Typically, water-to-wire efficiency or estimated power output for different flow and head conditions is provided for the hydropower products available in North America and parameters such as speed ratio (see section 2.6 for a discussion on speed ratio) are not discussed [18, 20, 29, 30]. With no data on turbine efficiency available to the user, proper system design for optimal performance (maximum power output) is much more difficult.

2.3.2 Electrical Generators

Both synchronous and asynchronous generators can be used for pico-hydro applications. Generator selection will depend on a number of factors including the generators available, cost, amount of power, type of electrical output (i.e. AC/DC, frequency, and voltage). The synchronous machines used are either conventional electromagnet or permanent magnet alternators (PMA) and the asynchronous machines are induction generators.

Induction generators offer a low cost, readily available method of converting mechanical energy to electrical energy [31]. With a few simple modifications, induction motors, commonly found throughout the world, can be made to generate electricity. Unlike conventional electromagnet alternators, over-speed is not usually a concern for induction motors because of their more resilient rotor design. Yet one more advantage of induction motors converted to generators is that they are well suited to generating AC power at the standard frequency and voltage since as motors

they were designed to run at those specifications. Induction generators, however, have brushes and slip-rings that require maintenance and have lower efficiencies than PMAs [24].

Conventional electromagnet alternators, such as those commonly used in automobiles, also offer a low cost, readily available method of electrical generation. They can be removed from old cars, refurbished, and used for pico-hydro. Car alternators are designed for battery charging meaning they will not be useful for outputting standard frequency and voltage to be used directly as AC power. Over-speed protection is required to prevent damage to the rotor at high rotational speeds, adding complexity to the system. Power is lost due to energizing the electromagnet in the core thereby reducing efficiency. This loss can be quite significant for low power applications.

Permanent magnet alternators, while more costly and less available than induction generators, offer high efficiency, in the neighborhood of 90% [24]. The electromagnet of a conventional electromagnet alternator is replaced with a permanent magnet that requires no electrical power to function. This modification eliminates the need for brushes and slip-rings that both electromagnet alternators and induction generators require. Over-speed is also generally not an issue since the rotor is a solid piece of material. On the downside, part load efficiency tends to be lower unless the speed is adjusted which would change the output voltage and current [32]. For systems connected to batteries, designing a set-up such that the PMA can operate at its

preferred speed for the expected power output should not pose a problem. Additionally, PMAs are now available with adjustable rotors that can change the magnetic flux and thus the peak operating conditions to better match the turbine [18].

2.4 System Design

The amount of power that can be produced from hydropower at a potential site depends on the volumetric flow rate Q of water and hydraulic head H available. The flow rate can generally be measured directly or estimated while hydraulic head is calculated using Eq. 2.1,

$$H = z + \frac{p}{\rho g} + \frac{v^2}{2g}, \tag{2.1}$$

where z is the vertical distance from datum (typically the turbine elevation), p is pressure, ρ is density, g is gravitational acceleration, and v is mean velocity [33]. Equation 1 was derived from Euler's equation and assumes a steady, incompressible, inviscid flow along a stream line. Any consistent unit system can be used for Eq. 1 as well as the other equations; however, the SI unit system is certainly the simplest.

The design process begins at the forebay, where Eq. 1 reduces to the elevation term only. We refer to the head at this location as the gross head H_g. From the forebay, the water must be carried downhill, to the powerhouse, by the penstock. Frictional forces in the penstock cause energy losses resulting in lower head at the downstream end of the penstock termed net head H_n, defined by Eq. 2.2 [33],

$$H_n = H_g - \Sigma H_l \,, \tag{2.2}$$

where ΣH_l is the sum of all head losses in the penstock and manifold.

Head loss is made up of major and minor losses caused by viscous forces in the pipe and secondary flow structures resulting from changes in direction and geometry of the flow, respectively. For penstock optimization, only major losses need to be considered since minimizing minor losses tends to reduce costs (whereas minimizing major losses by increasing pipe diameter increases costs). Neglecting minor losses, H_l can be found using the Darcy-Weisbach formula [34],

$$H_{l,major} = f\frac{l}{d}\frac{v^2}{2g}, \tag{2.3}$$

where f is the roughness coefficient (found on the Moody Diagram), L is the pipe length, D is the inside diameter, and v is the water velocity (through the pipe). The mean velocity of the water in a pipe (or jet) is given by,

$$v = \frac{Q}{A}, \tag{2.4}$$

where A is the cross sectional area of the flow.

When minor losses do need to be accounted for, there are several approaches that will lend useful results; one such method is to define a loss coefficient K_L that can be substituted into Eq. 2.3 as,

$$H_{l,minor} = K_L \frac{v^2}{2g}. \tag{2.5}$$

Loss coefficients for various common fittings and have been determined experimentally and are available in tables [34].

Once net head has been determined, it can be substituted into Eq. 2.1 along with Eq. 2.4. Equation 2.1 can then be simplified and solved for jet diameter. The resulting equation can be solved for diameter and is given as,

$$d_j = 2\left(\frac{Q}{n_j \pi}\right)^{1/2} \left(2gH_n\right)^{-1/4}, \tag{2.6}$$

where n_j is the number of jets. The nozzle(s) selected should be sized as close to the ideal jet diameter as possible or slightly smaller. Equation 2.6 neglects any head losses in the nozzles however these are typically insignificant for determining jet diameter (on the order of a 0.1% difference).

With net head and flow rate known, the amount of power in the water, referred to as hydraulic power $\dot{W}_h$, can be determined by [33],

$$\dot{W}_h = \rho g Q H_n. \tag{2.7}$$

To estimate the final system power output, efficiency values for the nozzles, turbine, and generator can be assumed. Thake provides reasonable values for each [24].

Table 2.3. Various nozzle types with associated velocity coefficients (adapted from Thake [24].

Nozzle Type	Velocity Coefficient
60° rounded nozzle	0.97
14° tapered nozzle	0.98
Sharp edged orifice	0.98
Rounded orifice	0.97

Limited generator options and specific input requirements mean generator selection takes precedence over other components, namely the turbine. The generator criteria depend heavily on the end use of the electrical power. Two types of machines are commonly used for electrical generation in pico-hydro schemes: asynchronous and synchronous.

Asynchronous AC induction motors are often converted to generators because of their availability and reliability [35]. These machines must be operated at a particular speed to generate the required frequency and voltage. If the turbine is to be directly coupled to the generator, it will have to operate at the same speed. Induction generators can be made from induction motors which are found in every country.

The other type of generator that is commonly used, the synchronous generator, is often a permanent magnet generator. Permanent magnet machines are generally used to supply DC power to a battery bank where it can be stored for later use. For DC power, the machine speed will not impact power quality but permanent magnet generators tend to become less efficient at higher speeds making it advantageous to operate at lower speeds. While alternators are common around the world because of

their use in cars, permanent magnet alternators are a specialty item used only when efficiency is particularly important and may be more difficult to find in a developing country. Regardless of the type of generator selected, shaft speed is likely to be determined by the generator.

For turbine selection, turbine type, speed ratio, and jet diameter must be considered. This thesis is primarily concerned with Turgo and Pelton turbines which are both impulse turbines. In the case of Turgo and Pelton Turbines, speed ratio, the ratio of the turbine speed to jet velocity, is defined as,

$$x = \frac{N\pi(PCD)}{60v_j} \tag{2.8}$$

where N is the turbine (or shaft) speed in revolutions per minute (rpm) and PCD is pitch-circle-diameter. Best efficiency is achieved with a speed ratio of about 0.45-0.50 for Pelton turbines [13, 24]. The literature provides no information how Turgo turbine efficiency varies with speed ratio. In the case of a Pelton turbine, empirical studies have demonstrated that a jet diameter exceeding 11% of the PCD of the turbine will decrease peak turbine efficiency [24]. Above this jet diameter threshold, the water cannot flow efficiently though the cups and the jet is likely to interfere with the cutout located at the outer edge of the cups. Figure 2.9 shows the cutout on of Pelton turbine.

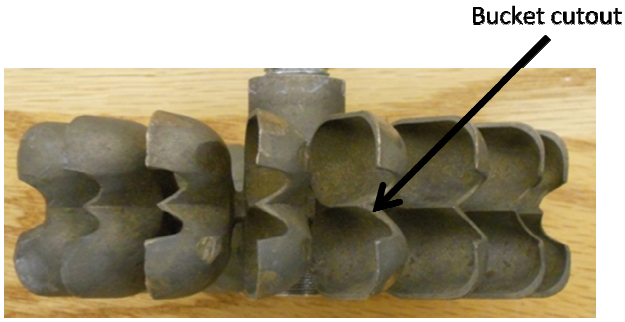

Figure 2.9. Photo of a 100-mm Pelton turbine showing the bucket cutout.

Turgo turbines are not quite as restrictive when it comes to jet diameter because of the cup geometry and water flow path. Jet diameter should not be so large such that part of the jet misses the turbine as this would reduce the amount of energy transferred from the jet to the turbine.

Turbine performance can be quantified by determining the power of the turbine, which is the same as the shaft power, defined by,

$$\dot{W}_s = 2\pi\tau\omega, \tag{2.9}$$

where τ is shaft torque and ω is the shaft speed in radians per second. Turbine efficiency η_{turb}, which measures how efficiently power is transferred from the jet to the turbine, can then be found using Eq. 2.8,

$$\eta_t = \frac{\dot{W}_s}{\dot{W}_j}. \tag{2.10}$$

Generator performance can be characterized in much the same way, by finding the ratio of power out to the power in. The power out, referred to as electrical power $\dot{W}_{elec}$ is simply the product the voltage across the generator terminals *V* and current through the circuit *I*, as given by

$$\dot{W}_{elec} = IV. \tag{2.11}$$

The efficiency with which the electrical generator converts mechanical shaft power into electrical power, defined as generator efficiency η_{gen}, can then be found by

$$\eta_{gen} = \frac{\dot{W}_{elec}}{\dot{W}_t}. \tag{2.12}$$

2.5 Specific Speed

A dimensionless parameter, specific speed, has been defined for turbines, to allow for comparison between different operating conditions and turbine dimensions. The method of repeating variables [34] dictates that there should be four dimensionless turbine parameters: the Head, Capacity, and Power coefficients and turbine efficiency [34]. For turbine applications where the flow is turbulent and the Reynolds numbers are fairly close together, dynamics similarity between different operating conditions and turbine dimensions is reasonable, thus Reynolds number can be ignored [34]. Additionally, the Head and Capacity coefficients are both approximately functions of the Power coefficient [34]. The independent parameter, Power coefficient, can be combined with one of the dependant parameters, the Head

and Capacity coefficients, to cancel out the turbine dimension. The result is a new parameter, specific speed.

Some controversy exists in the literature as to the usefulness of specific speed to nondimensionalize the operating conditions: rotational speed, head, and flow rate, to allow for comparison of geometrically similar turbines. Impulse turbine efficiency depends much more heavily on speed ratio than specific speed so specific speed is often ignored [24]. For reaction turbines, it seems that specific speed is useful since turbine efficiency does depend heavily on the parameters nondimensionalized in specific speed. Specific speed is defined as [33],

$$N_{s,1} = \frac{NQ^{1/2}}{(gH_n)^{3/4}}, \tag{2.13}$$

where N is the turbine rotational speed in rpm, Q is the volumetric flow rate, and H is the head. An alternative nondimensional specific speed that is written in terms of turbine power $\dot{W}_t$ rather than Q *[34]*,

$$N_{s,2} = \frac{N(\dot{W}_t)^{1/2}}{\rho(gH_n)^{5/4}}. \tag{2.14}$$

To maintain nondimensionality in both Eq. 2.13 and 2.14, consistent units must be used; however, more convenient units are often used and the density and gravity terms may be dropped, yielding a dimensional version of specific speed [36],

$$N_{s,3} = \frac{N\left(\dot{W}_t\right)^{1/2}}{\left(H_n\right)^{5/4}}, \tag{2.15}$$

where the units are $\frac{(rpm)(kW)^{1/2}}{(m)^{5/4}}$.

To characterize turbines, specific speed is most commonly found for the best efficiency point. Impulse turbines tend to fall at the lower end of the specific speed scale, with reaction turbines at the higher end. Since specific speeds for impulse turbines tend to fall within a fairly narrow range compared to those of reaction turbines, it is unnecessary to use specific speed to select an impulse turbine. Using the units of Eq. 2.15, specific speeds for impulse turbines tend to be less than 70; whereas, reaction turbines go up to approximately 1000.

2.6 Speed Ratio

Impulse turbine efficiency depends heavily on one operating parameter in particular, the speed ratio of the turbine and jet, defined as,

$$x = \frac{U}{v_j \cos(\gamma)}, \tag{2.16}$$

where v_j is the mean jet velocity, U is the tangential speed of the turbine at its PCD, and γ is the jet angle. Theoretically, the turbine efficiency will peak when $x=0.5$; in practice, the ideal speed ratio tends to be slightly less than 0.5, in the range of 0.42-0.48 [24].

The theoretical maximum is found by setting up a finite control volume analysis which can be simplified to the Euler turbomachine equation for a turbine and dotted with the angular velocity, resulting in an equation for power. In scalar form, that equation is,

$$\dot{W}_s = \dot{m}U\left(v_{i,t} - v_{e,t}\right), \tag{2.17}$$

where $\dot{m}$ is the mass flow rate of water, and the v_t terms are the velocity components tangent to the radial plane of the turbine at the influent (*i*) and effluent (*e*) locations [33].

In the case of the Pelton turbine, $v_{i,t}$, the tangential velocity of the jet entering the turbine, is simply v_j-U since the jet is in the radial plane. At the turbine exit, the tangential jet velocity is given by,

$$v_{e,t} = U + \left(v_j - U\right)\cos\left(\beta_e\right) \tag{2.18}$$

where β is the angle measured from the radial plane at which the water exits the turbine, as shown in Fig. 2.9(a). By substituting these terms into the power equation, Eq. 2.17, that equation becomes

$$\dot{W}_s = \dot{m}U\left(v_j - U\right)\cos\left(\beta_e\right). \tag{2.19}$$

Then, taking the derivative of Eq. 2.19 with respect to U and setting it equal to zero, it turns out peak power occurs at $v_j/U=0.5$. Figure 2.10 shows a schematic view of a

Pelton turbine blade and velocity vector diagram. The subscript *r* refers to the rotating reference frame.

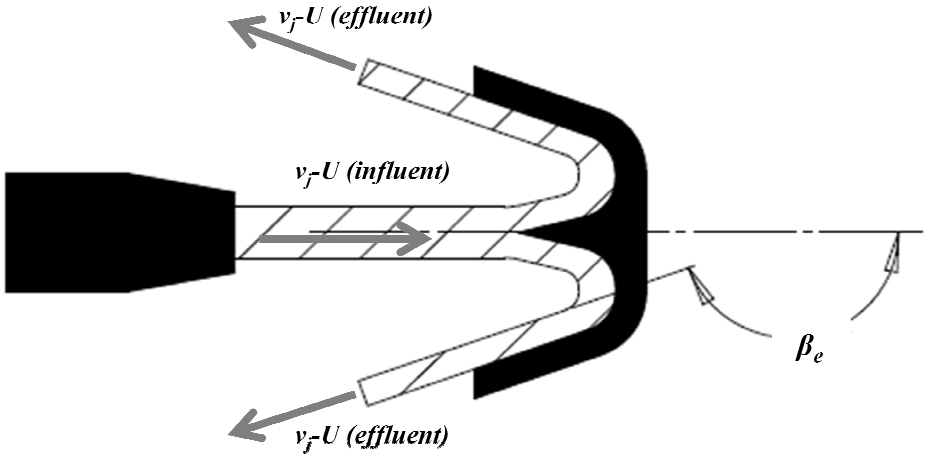

(a)

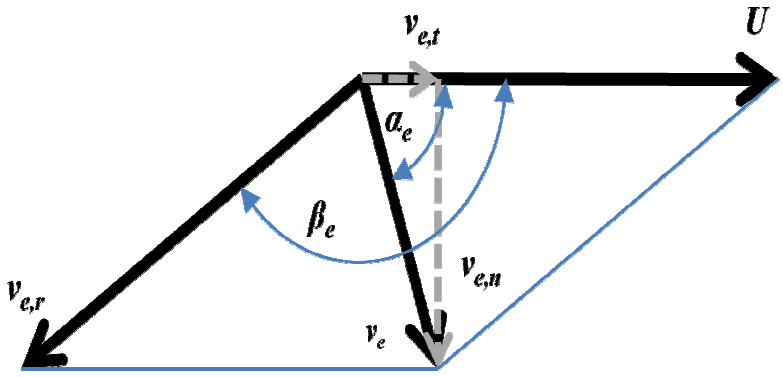

(b)

Fig. 2.10. Water flow through a Pelton turbine blade. (a) Cross section of a Pelton turbine blade with jet impingement in the rotating reference frame, and (b) velocity diagram of the effluent flow of a Pelton turbine blade showing the translation from rotating reference to absolute frame.

For the Turgo turbine the tangential jet velocities at the entrance and exit can be determined by once again summing velocity vectors. Figure 2.11 shows a schematic view of a Turgo turbine blade and a velocity vector diagram for the water entering and exiting the turbine. The water jet enters the turbine at some jet angle α.

Figure 2.11. Water flow through a Turgo turbine blade. (a) Cross section of a Turgo turbine blade with jet impingement in the rotating reference frame, (b) velocity diagram of the influent flow of the turbine blade showing the translation from rotating reference to absolute frame, and (c) velocity diagram of the effluent flow of the turbine blade showing the translation from rotating reference to absolute frame.

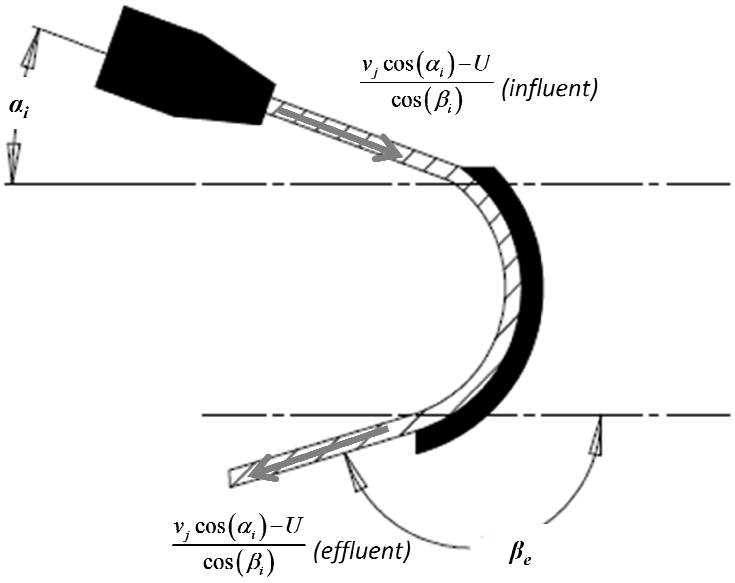

(a)

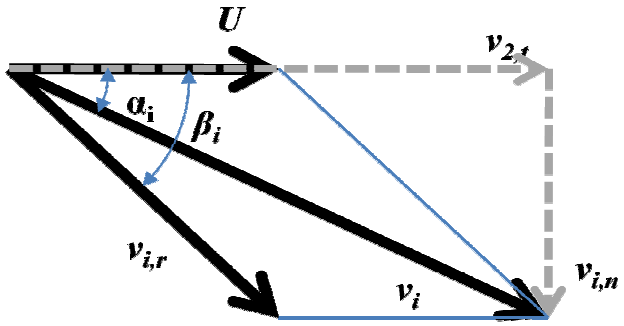

(b)

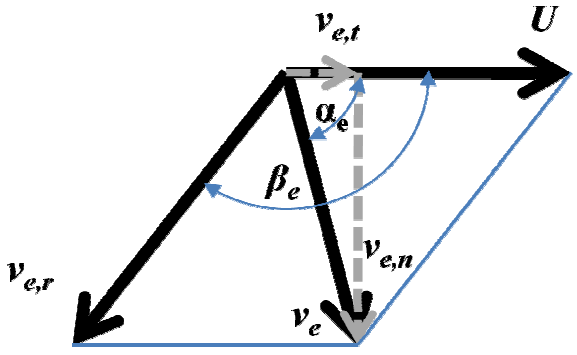

(c)

Figure 2.11

Based on the velocity vector diagrams, the influent and effluent tangential water velocities are found to be,

$$v_{i,t} = v_j \cos(\alpha_i), \tag{2.20}$$

$$v_{e,t} = \frac{v_j \cos(\alpha_i) - U}{\cos(\beta_i)} \cos(\beta_e) + U \quad . \tag{2.21}$$

Equations 2.20 and 2.21 can then be substituted back into Eq. 2.17 to solve for power.

2.7 Turgo & Pelton Turbine Comparison

Ideal peak turbine efficiency, as defined by Eq. 2.10, drops slightly for the Turgo turbine compared to the Pelton turbine due to the jet angle and the exit angle of the water leaving the cups. According to the velocity vector model presented, at jet angle of 0° (like a Pelton turbine) and an exit angle that is also 0°, a maximum of 100% efficiency could be obtained. Realistically, the water cannot exit the turbine at the same angle it enters due to geometric constraints so previous tests have shown that a 15-20° [24, 34] exit angle provides the best performance. The corresponding maximum turbine efficiency for such a shift in exit angle is 97.0-98.3%. For a Turgo turbine with a jet angle and exit angle of 20°, the maximum possible efficiency is reduced to 96.6%, only slightly lower than the Pelton turbine with the added benefit of a much larger maximum flow rate of water through the turbine since the water exits on the opposite side from where it enters the turbine. Other sources of energy loss not accounted for in this model such as viscous forces, windage losses, and those resulting

from the changing jet impingement location on the turbine blades (due to the rotation of the turbine), will reduce the actual operating efficiency of both turbine types. The model, however, suggests that the associated differences in efficiency should not be significant for pico-hydro applications.

Chapter 3 – Pico-hydro Background

To put pico-hydro in context, this section begins by providing an overview of how small-scale hydropower is being used around the world. Then a summary of recent research aimed at improving the functionality of pico-hydro will be discussed.

3.1 Case Studies

Small-scale hydropower has been implemented around the world to address the lack of access to reliable electricity in many rural communities as well as to produce renewable energy in places where grid power is not available. Hydropower is a well-established technology with a proven track record of reliable operation and is among the most cost effective sources of electricity for mini-grid applications. In order for small-scale hydropower to be effective in less developed countries however, efforts must be made to introduce rural communities to the technology, demonstrate its effectiveness and make sure it is economically feasible. The same can be said of more developed countries; pico-hydro must be shown to be a reliable and economical renewable power source.

3.1.1 Asia and the South Pacific

Across Asia and the South Pacific, small-scale hydropower has been used to bring electricity to rural communities for decades in some regions and continues to grow today. Organizations have been at work in Nepal and India since the 1970s and 80s [23, 37] constructing small scale hydropower sites for mini-grid electrical systems. More recently, projects in other countries where a need for low-cost electrical power exists along with the water resources necessary have started to appear, including

projects in Lao PDR, Afghanistan, Pakistan and several other Middle Eastern countries have begun to spring up. The schemes are usually designed to supply electricity to rural residents in small communities where connection to a national grid is not feasible. Mini-grids powered by hydropower turbines can be set up in such areas to supply power to a few hundred or a few thousand residents to power lights and small appliances such as radios. A summary of some of the projects that have been documented in case studies is presented in Table 3.1 and a map of the sites is provided in Fig. 3.1. The numbered markers represent case study sites.

Table 3.1. List of documented small-scale hydropower projects in Asia.

Location	Capacity (kW)	Head (m)	Flow rate (l/s)	Turbine type	Comments
Thalpi, Nepal [38]	0.165	2.1	25	Propeller	Used to provide lighting to 30 households
Kholis, Nepal [38]	1.1	2.5	80	Propeller	56% efficiency, used for lighting and heating water
Padisaw, Afghanistan [39]	7	7	Not available	Not available	Provides lighting for 35 households
Kushadevi, Nepal [40]	4.4	100	13.5	Pelton	Designed for as low as 9 l/s in the dry season
Karimi, India [37]	50	70	130	Cross flow	Provides power to 225 households
Kampung Tuil, Malaysia [22]	5	40	28.4 (est.)	Not available	Flow rate estimated based on head and power output
Wangan Aji, Indonesia [41]	100	11.12	1420	Propeller (2x)	Provide power to a rural village and school
Northern Samar, Philippines (Tangan-Ayan)[42]	6	4.2	240	Propeller	Supplies power to 60 households as a part of a hybrid system
Northern Samar, Philippines (Epaw) [42]	3.2	2.8	190	Propeller	Supplies power to 44 households as part of a hybrid system

Fig. 3.1. Map of documented small-scale hydropower projects in Asia.

3.1.2 Africa

Small scale hydropower has been widely used in Africa as well, where rural electrification rates are some of the world's lowest [3]. As in Asia, mini-grids supplied by hydropower are often the most economical way to supply power to rural communities given sufficient water resources. A number of successful projects in Kenya have been used as case studies to help promote the available hydropower technology and demonstrate how it can be implemented with hopes that the concept will spread to other parts of the continent. Interest in small-scale hydropower now exists in several other African countries including Cameroon, South Africa, Zimbabwe and Tanzania just to name a few [43-46]. Table 3.2 lists some of the projects in Africa along with details about each and Fig. 3.2 shows a map of the sites.

Table 3.2. List of documented small-scale hydropower projects in Africa.

Location	Power (kW)	Head (m)	Flow rate (l/s)	Turbine type	Comments
Kathamba, Kenya [47]	1.1	28	8.4	Pelton	Powers 65 households
Thima, Kenya [48]	2.2	18	28	PAT	Powers 110 households
Tungu-Kabriri, Kenya [43]	14	13	200	Not available	Powers 300 households (3000 people), likely used a propeller turbine or a PAT
Crammond, South Africa [44]	40	12	400	Not available	Drives a centrifugal pump for irrigation, likely used a propeller turbine
Svinuray, Cashel Valley, Zimbabwe [44]	10	100	20	Pelton	Drives generator and grinding mill, flow rate estimated using 50% system efficiency
Sioma, Zambia [7]	46.1	10	626	Propeller	Powers a wood shop, clinic, school and 200 households, custom built turbine

Fig. 3.2. Map of documented small-scale hydropower projects in Africa.

3.1.3 Latin America & the Caribbean

Many Latin American and Caribbean countries are prime candidates for small-scale hydropower systems with adequate water resources and low electrification rates. Cuba, Peru and Columbia among others have installed hydropower schemes for mini-grid systems to supply the need for electricity in rural areas [49]. A partial list of small-scale hydropower projects in Latin America is provided in Table 3.3 with a map of the sites provided in Fig. 3.3.

Table 3.3. List of documented small-scale hydropower projects in Latin America.

Location	Power (kW)	Head (m)	Flow rate (l/s)	Turbine type	Comments
Camata, Bolivia [50]	27	Not Available	Not Available	Pelton	70 households and agro-processing facility
Cambamontera, Peru [41]	15	89.5	35	Pelton	60 households
Cajamarca, Peru [51]	35	50	110	Pelton	85 households
San Jose de Bocay, Nicaragua [52]	3	6.35	100	Cross-flow	Powers to a coffee and corn plantation, power estimated for 50% system efficiency

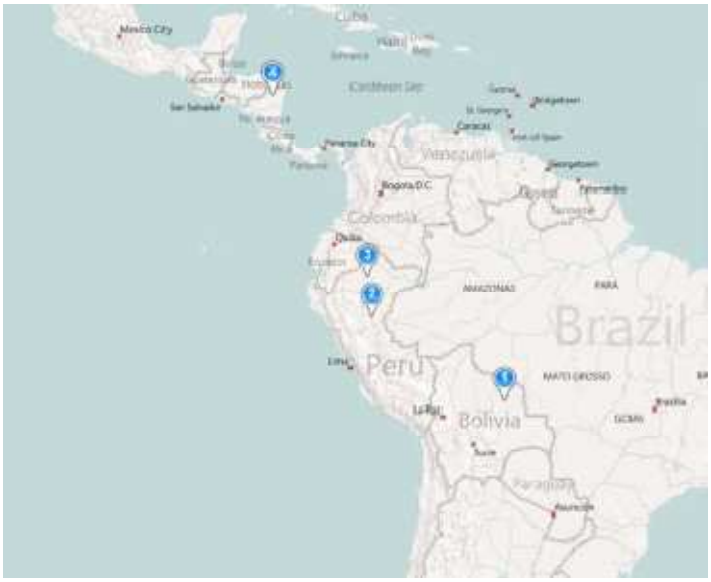

Fig. 3.3. Map of documented small-scale hydropower projects in Latin America.

3.1.4 Developed Regions

In the more developed countries of North America, Europe and Australia and New Zealand, low rural electrification rates tend to be less of a driver behind small-scale hydropower; rather, environmental concerns tend to be the reason to explore alternative forms of power generation with grid connection in mind. Several cities including Gresham, OR, Wellington, NZ and Boulder, CO have looked into using excess head from the cities' water and sewage systems to drive turbines to generate electricity. Boulder has already taken the next step by installing several turbines that are producing power [50-52]. Using water released from existing reservoirs is another renewable energy concept being implemented [53, 54]. Occasionally, new small-scale hydropower installations have been considered in areas where the natural water resources and a desire for clean sustainable electricity generation exist but no reservoir is present [15, 55-58]. While the emphasis on the majority of these projects is to generate renewable power at a cost that is competitive with conventional utility rates, occasionally mini-grid generation is the only feasible method of supplying power to rural communities [59]. A partial list of case studies in the developed regions is provided in Table 3.4.

Table 3.4. List of documented small-scale hydropower projects in developed regions.

Location	Power (kW)	Head (m)	Flow rate (l/s)	Turbine type	Comments
Gresham, OR [51]	50	Not available	Not available	Not available	Proposal uses hydro turbines to replace pressure reducing valves in water system at 12 sites
Oregon City, OR [60]	2.4	36.6	7.65/15.3	Pelton	Feasibility study, storm drain system, Variable 2/4 jet Pelton
Oregon City, OR [60]	5.4	27.4	50.4	Pelton	Feasibility study, storm drain system, Variable 2/4 jet Pelton
Beaver Run, PA [54]	30	26 (est.)	238	Not available	Installed at existing reservoir, likely a Fransis turbine, estimated head based on 50% system efficiency
Pawnee, OK [61]	53.8	4.44	2477	Not available	Feasibility study, likely to use a Francis turbine, estimated power based on 50% system efficiency
Hoopa Valley, CA (Hostler Creek) [62]	19	11.9	283	Not available	Feasibility study
Salt Springs Island, BC (Fulford Creek) [58]	9.2	40	80	Not available	Feasibility study
Salt Springs Island, BC (Big Creek) [58]	6.3	80	21	Not available	Feasibility study
Newtownards, Northern Ireland, UK [63]	56.4	13.55	500	Kaplan	Feasibility study, power estimated based on 85.5% system efficiency)
Rhyd Hall, Wales, UK [57]	1.77	62.8	4.7	Turgo	Feasibility study, used for education and power production
Brideswell, Scotland [55]	3.7	18.5	60	Turgo	Installed, 4 jet Turgo
Dorset, UK (Cards Mill) [53]	6.4	3.1	405	Not available	Feasibility study for rivers
Dorset, UK (Lordsmead Mill) [53]	6.2	2.85	416	Not available	Feasibility study for rivers
Wellington, NZ (Porirua Low-Level Reservoir) [52]	31.5	40	97.2	PAT	Feasibility study to use micro-hydro for pressure reduction in water system
Maungapohatu, NZ [59]	6	117	10	Pelton (2x)	Feasibility study to supply power to a remote village within a national park
Tauranga, NZ [64]	14	22	100	Turgo (2x)	Feasibility study to supply power to a farm and power grid

Fig. 3.4. Map of documented small-scale hydropower projects in developed regions.

3.2 Modular System Design

One of the most important research areas in recent years has been in developing methods for streamlining the design process by minimizing the site specific work required for each installation. Charts have been developed to aid in reaction turbine selection based on specific speed [16]. Turbines are available for a range of specific speeds of up to 20 kW, above which more site specific design tends to be cost effective. The use of pumps-as-turbines (PAT) has also been explored with several systems already built [31]. PATs are relatively efficient, low cost, and readily available; additionally, they are generally already attached to a motor that can be wired to work as a generator. An instruction manual for designing PAT systems has also been developed [26], further streamlining the design process. One of the issues that has been tackled recently related to PATs is determining operating curves

experimentally that can be correlated to the manufacturer's pump operating curves [65]. The Pico Power Pack, consisting of a Pelton turbine directly coupled with an induction generator, has been developed for a wide range of high head applications [35]. An instruction manual describes, in step-by-step detail, how to design the facility from start to finish [25]. Even with modular systems, proper site assessment is important. Recent work has investigated how the site assessment process can be streamlined by the use of software programs such as EPANET to model seasonal flow variations and estimate head losses for pipe networks [15].

3.3 Hybrid Systems

When the water resources are not present to fully meet the power demand at a particular site with hydropower, it may be cost effective to design a hybrid system that combines two or more types of power generation. Pico-hydro may be combined with wind, solar, biomass, or battery systems to meet the demand. For hybrid systems to be economical and meet the power demand, the components must be optimized to account for peak and average loads and variations in resources. Developing tools, such as the software package HOMER, to aid in design optimization has been a focal point for research. So far, hybrid systems have been developed for sites in Cameroon [66, 67] and India [68], where the wet, cloudy season and a dry, sunny season, experienced by many equatorial regions, make hydro and solar a complimentary match. HOMER is an open source software package available from the US National Renewable Energy Laboratory [69].

3.4 Low-head Pico-hydro

Historically, low head pico-hydro had been largely neglected when compared to medium and high head due to higher initial costs resulting from lower power density. Demand for electricity in developing countries, the abundance of low head water resources, and a push toward renewable energy has made these types of schemes more appealing in recent years. Two thrust areas in low head pico-hydro research have been turbine and case design and modular system design.

For low-head pico-hydro, reaction or cross-flow turbines are typically used [23]. While cross-flow turbines are cheap, easy to manufacture, and work for a wide range of flow conditions, they have low peak efficiencies. The lower head already necessitates a higher flow rate, meaning larger more expensive penstocks; low turbine efficiency further exacerbates the low power density issue. Reaction turbines on the other hand, can be extremely efficient, if properly designed, but only for a narrow range of operating conditions. Scaling large reaction turbines down to pico-hydro scale is impractical due to cost and manufacturing constraints [44]. Reaction turbines generally require complicated turbine housings that involve shaft seals and guide vanes to direct the flow into the turbine that cannot be readily manufactured inexpensively with simple methods. To address the need for low cost, efficient low head turbines that can be manufactured locally, researchers have developed a series of turbines that do not require complicated housings [36, 44, 70]. Computational Fluid Dynamics (CFD) modeling and experiments are being used, with the hope of raising

turbine efficiency from the 50% range seen on the market (as of 2009) to above 80%, for developing new turbine designs [71].

3.5 Medium-head Pico-hydro

Medium-head is often lumped in with either low or high-head for simplicity though there are some distinctions that should be considered. While Pelton and cross-flow turbines can and are used for medium-head conditions, other options are at times more economical. This is the region where Turgo turbines can be most effective. Recent work on Turgo turbine design using CFD modeling has brought some attention to the use of Turgo turbines for pico-hydro [72] though published literature on the subject is limited. Cross-flow turbines may also be used at the lower end of the medium head range, as well as the PATs discussed in section 3.2. Some recent studies have focused on optimizing turbine selection by weighing all of the advantages and disadvantages of each turbine type [31, 73]

3.6 High-head Pico-hydro

High head tends to be a more mature technology than low head since it tends to be more economical; although, there are still areas where research is being done. Turbine flow modeling, manifold and injector flow modeling, design for local manufacturability, and technology dissemination.

Due to the irregular geometry of Pelton turbine blades and rotation, visually observing the flow of water through the turbine is difficult. Recent advances in computer processor power have allowed for more accurate modeling of the flow [74-76]. In the past, Pelton turbines had been designed using more of a trial and error approach, where a prototype was constructed, tested, and improved upon in successive prototypes. Over time, fairly high efficiency designs were built, though the mechanisms that made one design superior to another were not well understood. Researchers are now using computer modeling to design and optimize turbines before they are even built, saving valuable time and money [75]. Although very efficient Pelton turbines are already available on the market today, there is still room for efficiency improvements in the Pelton turbines that are readily manufactured. For example, some of the commonly used Pelton turbines were found to have efficiencies in the 70% range, leaving room for further improvement [13].

CFD is also being used to aid the design of multi-jet Pelton turbine systems [76]. More jets, which allow for higher flow rates and thus greater power output, necessitate a better understanding of the flow through the turbine and how manifold design impacts water jets. For single or multi-jet systems, jet quality can have a major impact on turbine efficiency [77]. With the use of CFD, manifolds can be designed so as to minimize secondary flow structures in the water and deliver a high quality jet to the turbine.

3.7 Electronics

Electronic load controllers (ELC), first used with pico-hydro in the 1980s, have provided an effective means of regulating voltage and current of off-grid electrical systems without the use of batteries. A need still exists for updated, more versatile, low-cost ELCs that can deliver high quality power at any operating condition [16]. Recent research has focused on developing ELCs that can meet the needs of pico-hydro by eliminating mechanical parts from the speed control system, resulting in simpler, more reliable designs that can effectively deal with both resistive and reactive electrical loads [78, 79]. Work is also being done with ELCs that regulate water flow to improve performance and reliability in situations where it may be advantageous to conserve water when less power is required [80].

Generator design is another area of research interest for pico-hydro. For systems under 1 kW, permanent magnet, synchronous AC generators are often used because of their high efficiency and reasonable cost [81]. Above 1 kW, AC induction generators are typically more cost effective, despite their lower efficiency. New synchronous machines have been proposed that use a different geometry design that will allow for higher efficiency power generation above 1 kW while keeping cost and machine size down [81]. The new generators are similar to those currently used for wind power in developing countries with great success [82].

3.8 Laboratory Test Systems

A number of laboratory scaled test fixtures have been constructed for carrying out experiments with small-scale hydro turbines and educating students in recent years [83-86]. The Pico Turbine Laboratory in Nepal is designed for reaction turbines typically used for low head pico-hydro applications and is used for testing vertical-axis axial-flow turbines from 0.4-2 kW [86]. Few details are provided on the test set-up used by Singh and Nestmann but it was used for a vertical-axis propeller turbine at around 1.5 kW [85]. For impulse turbine testing, Agar and Rasi describe in detail a test fixture designed to operate with Pelton turbines in Finland [83]. The test rig was constructed primarily for educational purposes, as it operates at very low power (only a few watts). Results obtained clearly demonstrate the relationship between speed ratio and efficiency. A much more robust system was developed by Baines and Williams that can accommodate more practical power levels for pico-hydro and Pelton turbines from 100 to 180 mm pitch-circle-diameter in the UK [84]. Turbines already on the market and new turbine designs can be tested to verify reasonable efficiency across a range of flow and head conditions. Local testing facilities, in the regions where pico-hydro is being implemented would be useful for verifying the performance of locally manufactured turbines.

Chapter 4 – Experimental Methods

4.1 Test Fixture Design

For the experiments documented in this thesis, a laboratory test set up, shown in Figs. 4.1 and 4.2, was constructed to simulate a typical pico-hydro scheme. The system consists of a vertical axis impulse turbine directly coupled with a DC-540 permanent magnet alternator (PMA, Wind Blue Power, New Strawn, KS) and a 2 hp centrifugal pump (MP Pumps, Fraser, MI) driving the flow of water to create a water jet that turns the turbine. A pump performance curve is included in Appendix B. The set up can accommodate both Pelton and Turgo turbines up to a pitch-circle-diameter (PCD) of 170 mm. Currently, a 100-mm PCD brass Harris Pelton turbine (ABS Alaskan, Fairbanks, AK), a 131 mm PCD plastic Turgo turbine, and a 169-mm PCD plastic Turgo turbine (Hartvigsen-Hydro, Kaysville, UT) have been tested. The turbine and nozzle are located inside an inverted catch basin that contains the water leaving the turbine. The generator is mounted on top of the catch basin on a bearing that allows the generator to spin freely about the shaft. Polyvinyl chloride (PVC) pipes and tubing have been used for the flow loop. An isolation valve is located in the flow loop to stop the water flow without turning the pump off and a ProFile2 flow control valve (Hayward Industrial Products, Clemmons, NC) can be installed to adjust the flow rate.

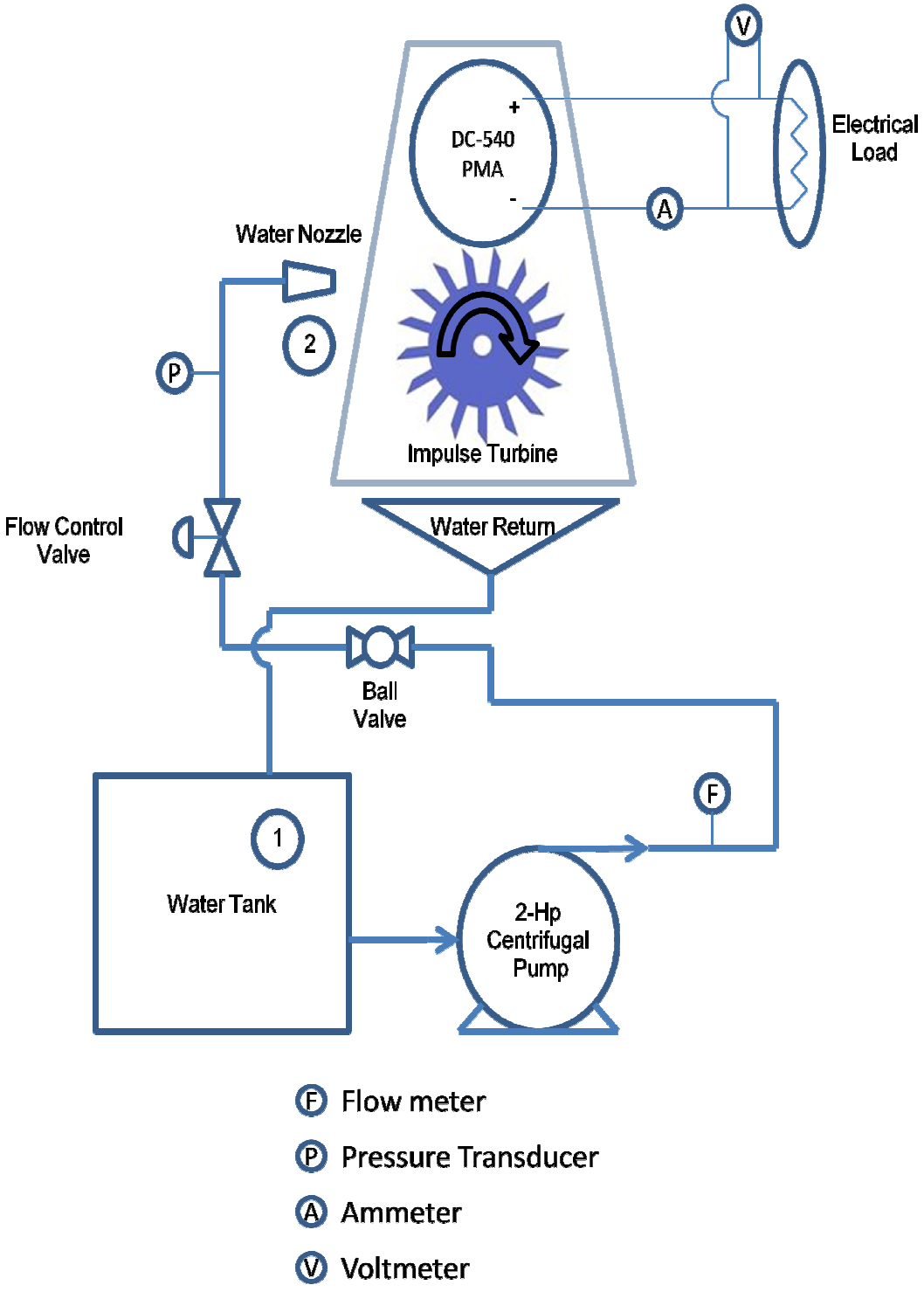

Fig. 4.1. Schematic of laboratory-scaled test fixture.

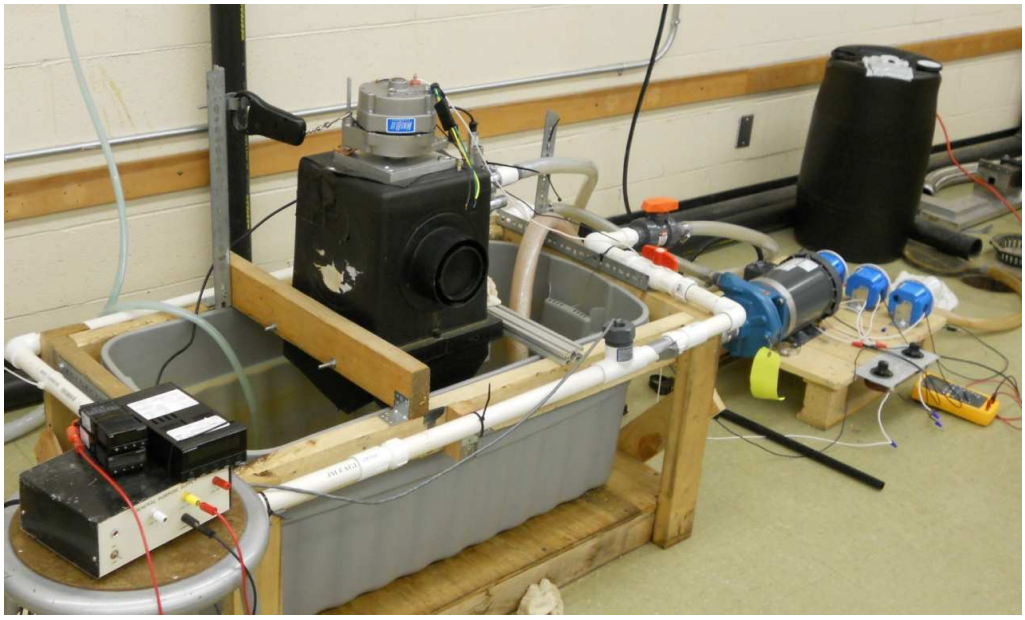

Fig. 4.2. Pico-hydro lab test fixture.

Various instruments have been installed throughout the system in order to characterize the performance of the principle components, the nozzles, turbine and PMA. An FP-7001A paddle wheel flow sensor with integrated temperature sensor (Omega Engineering, Stamford, CT), with a range of 0–50 gpm, measures the volumetric flow rate of water through the flow loop. Additionally, the flow loop pressure is measured using a PX309-050GV pressure transducer (Omega Engineering, Stamford, CT) over a range of 0–50 psig. A Fluke 189 (Fluke, Everett, WA) and a Model 982015 (Sears Hoffman Estates, IL) digital multimeter are used to measure voltage and current produced by the PMA. Shaft speed, ω_{rev}, is measured using a Model 461920 laser tachometer (Extech Instruments, Waltham, MA). A list of the instrumentation is provided in Table 4.1.

Table 4.1. List of instrumentation used for data collection.

Instrument	Instrument Range	Test Range	Graduations	Accuracy	Manufacturer
Paddle Wheel Flow Meter (gpm)	3-50	13-30	0.001	+/- 2% FS	Omega Engineering
Pressure Transducer (psi)	0-50	12-40	0.01	+/- 0.25% FS	Omega Engineering
Hanging Scale	0-50 lbs.	1 lb. 6 oz.-8 lb.	1 oz.	+/- 3 oz.	Berkeley
Laser Tachometer (rpm)	2-99,999	400-2000	0.1	+/- 0.05% Reading	Extech

A calibration was performed on the paddle wheel flow meter to reduce the uncertainty jet power and turbine efficiency. The calibration is discussed later in section 4.2. Factory calibrations were used for all other instruments used in data collection.

Water stored in a tank is pumped through the flow loop by the centrifugal pump. The water flows through the flow meter, isolation valve, flow control valve (if installed), and the nozzle. The pressure transducer is located just upstream of the nozzle. Downstream of the nozzle the water forms a jet which impinges on the turbine, thus transferring its kinetic energy to the shaft. The water then exits the turbine and returns to the holding tank where it is recycled back in to the flow loop. A schematic of the test rig is shown in Fig. 4.2.

4.1.1 Turbines

Three turbines have been selected for testing, a Pelton and two Turgo turbines. The Pelton turbine is a 100 mm PCD Harris Pelton turbine (ABSAK, Fairbanks, AK) made of bronze and cast as a single piece. The Turgo turbines are 131 mm and 169 mm PCD (Hartvigsen-Hydro, Kaysville, UT) respectively and are made of individually injection molded cups secured to a stainless steel hub. The turbines are pictured in Figs. 4.3 and 4.4.

Fig. 4.3. Picture of the 100-mm Harris Pelton turbine used in this study.

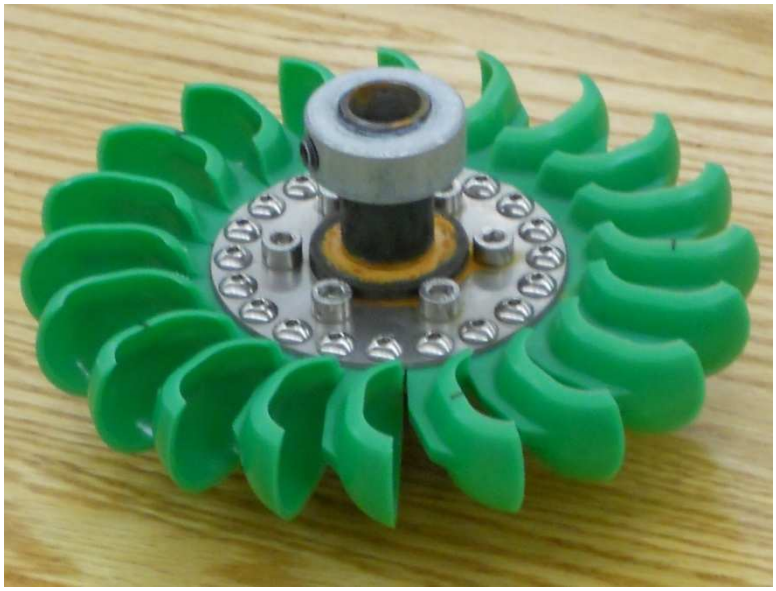

Fig. 4.4. Picture of the 133-mm Hartvigsen Hydro Turgo turbine used in this study.

4.1.2 Nozzle Mount System

A nozzle mount system was constructed to allow for variation in the nozzle position. Having the ability to adjust nozzle position is necessary in order to test different types and sizes of turbines and is also useful for fine tuning the jet alignment. The nozzle mount system constructed allows for four degrees of freedom: elevation, radial and tangential position, and nozzle angle. Additionally, the entire nozzle mount structure can be moved in relation to the turbine housing when large adjustments are necessary. Elevation is adjusted by moving the nozzle apparatus up or down on its vertical axis while radial adjustment are carried out by rotating the nozzle apparatus about the vertical axis. Tangential position is adjusted by moving the apparatus in or out along the tangent line of the turbine. Nozzle angle is measured in relation to the

horizontal plane using a Dasco Pro Angle Finder with a +/-1° resolution. A picture of the nozzle mount system is shown in Fig. 4.5.

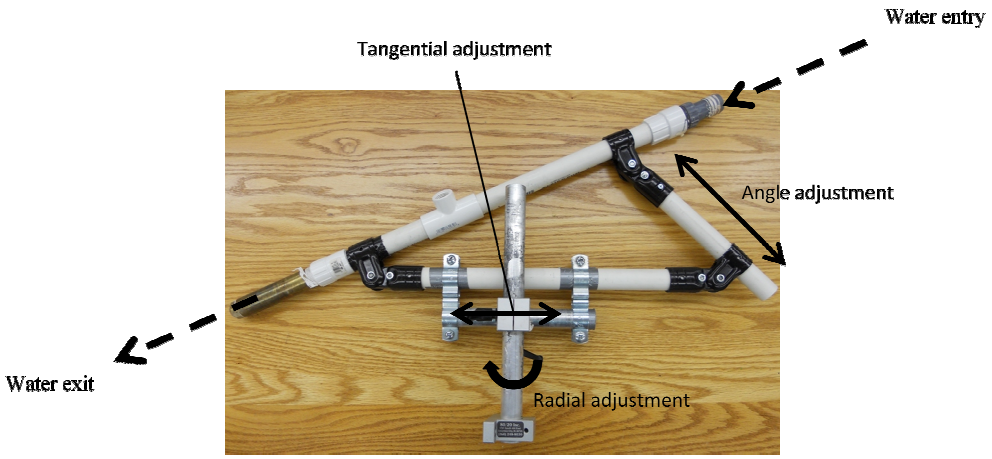

Fig. 4.5. Photo of the nozzle mount system with position adjustments and water flow path annotated.

4.1.3 Summary of Capabilities

Pelton and Turgo turbines of up to approximately 170 mm PCD can be tested in the test fixture for shaft speeds from 400 to 1900 RPM by varying the electrical resistance on the output circuit of the generator. A maximum of 350 W of hydraulic power can be delivered to the turbine and a maximum head of 29 m can be achieved. Currently, four nozzle sizes, ranging from 7.94 to 12.7 mm, can be used to produce different jet diameters and flow conditions. A flow control valve can also be installed to change the head and flow rate.

4.2 Data Reduction

Like a typical pico-hydro scheme, hydraulic head can be calculated at any location where elevation, pressure, and velocity are known using the head equation introduced in section 2.4,

$$H = z + \frac{p}{\rho g} + \frac{v^2}{2g}. \tag{2.1}$$

For the laboratory test set up used in this thesis the flow meter and pressure transducer can be used to directly determine net head, located upstream of the nozzle. Head losses in the system can then be used, along with Eq. 2.2, to determine gross head, the head at the pump outlet, which can be compared to the pump manufacturer's pump performance curve. The pump performance curve for the pump used here is available in Appendix B.

To find jet head H_j and jet velocity v_j, the head and velocity downstream of the nozzle, Eq. 4.1 and 4.2 are used,

$$H_j = C_v^2 H_n \tag{4.1}$$

$$v_j = C_v \sqrt{2gH_n} \tag{4.2}$$

For a turbulent flow, it is a reasonable assumption that velocity coefficient depends only on nozzle geometry. The velocity coefficient for a particular nozzle can then be found in a table. Nozzle efficiency is directly related to the square of velocity coefficient meaning it is also assumed. According to the literature [24], for a 60°

rounded nozzle $C_v=0.97$ and for a 14° tapered nozzle $C_v=0.98$. The brass nozzles used for this study all fall between these two geometries so $C_v=0.975$ was assumed. The plastic nozzles used for jet quality comparison have a lower velocity coefficient that can be approximated using the same method used to account for minor head losses in section 2.4. The result from that method estimates a velocity coefficient of about $C_v=0.82$.

Using the measured parameters discussed in the previous section and calculated jet head, the hydraulic power in the water jet, shaft power, and electrical power can be found for the system. Jet power can then be found by replacing the net head in Eq. 2.4 with jet head as shown in Eq. 4.3,

$$\dot{W}_j = \rho g Q H_j \tag{4.3}$$

where the flow rate Q is the same value used earlier. The power transferred to the turbine, and thus the shaft, can be found by relating the shaft speed ω and torque T using Eq. 4.4,

$$\dot{W}_s = \frac{2\pi T \omega}{60}. \tag{4.4}$$

For Eq. 4.4, shaft speed is in units of revolutions per minute (rpm). Shaft power is then converted to DC electrical power by the generator which can be found using Eq. 4.5,

$$\dot{W}_{elec} = IV, \tag{4.5}$$

where I is the current through the circuit and V is the voltage across the alternator terminals.

With jet power, shaft power, and electrical power known, the efficiency with which the turbine and generator convert power from one form to another can be found by taking the ratio of the power out to the power in to the two devices as shown in Eqs. 4.6 and 4.7,

$$\eta_t = \frac{\dot{W}_s}{\dot{W}_j}, \tag{4.6}$$

$$\eta_{gen} = \frac{\dot{W}_e}{\dot{W}_s}. \tag{4.7}$$

For impulse turbines, turbine efficiency is commonly plotted as a function of speed ratio since there is a strong relationship between the two. For PMAs, it is useful to plot generator efficiency as a function of shaft speed.

4.3 Uncertainty Analysis

Experimental uncertainties for all calculated values of power and efficiency were estimated to ensure the validity of the results. The method described by Kline and McClintock [87] for uncertainty propagation in single measurement experiments was used to account for uncertainty in the calculated values. The total uncertainty from a single measurement can be described by Eq. 4.8,

$$\theta_x = \sqrt{B_x^2 + \left(tS_x\right)^2}, \tag{4.8}$$

where B is the bias error, t is the student t-factor, S is the standard deviation, and the subscript x designates which parameter the uncertainty applies to. Combined, t and S are the random error. The t-factor is a measure of how much the distribution of a set of measured values differs from the standard deviation. For a large enough sample, more than 30, t can be taken to be 2. Standard deviations from different measurements that are input into an equation can be combined to find the standard deviation for the result using Eq. 4.9,

$$\theta_R = \sqrt{\sum_{i=1}^{n} \left(\theta_i \frac{\partial R}{\partial x_i} \right)^2} , \tag{4.9}$$

where $\partial R / \partial x_i$ is the sensitivity coefficient for a particular measurement. The estimated uncertainties for the salient calculated values are given in Table 4.2.

Table 4.2. Uncertainty estimates for notable calculated parameters.

Calculation	Nominal Range	Best Case Uncertainty	Worst Case Uncertainty	Major Contributor(s)
Net Head (m)	9.00-28.00	0.32%	0.98%	Pressure measurement
Jet Velocity (m/s)	13.0-22.8	1.04%	1.13%	Velocity coefficient assumption
Jet Power (W)	140-350	2.41%	2.75%	Velocity coefficient, Flow rate measurement, Net head calculation
Turbine Power (W)	100-300	4.08%	8.32%	Torque measurement
Electrical Power (W)	40-170	0.51%	5.30%	Current measurement, voltage measurement,
Turbine Efficiency	0.50-0.85	4.89%	8.93%	Turbine power, jet power
Electrical Efficiency	0.38-0.69	4.12%	8.47%	Turbine power, Electrical power
Combined Efficiency	0.19-0.60	6.29%	9.79%	Turbine efficiency, Electrical Efficiency
Speed Ratio	0.4000-0.5000	3.96%	3.97%	Jet velocity calculation, PCD measurement

Due to changing operating conditions in the system and number of measured parameters used in calculations, some of the calculated parameters have a wide gap between the best and worst case for uncertainty. Turbine power depends primarily on the measurement of shaft torque. Larger values of shaft torque result in lower turbine power uncertainty as a percent of the total value meaning higher power and higher torque produce lower uncertainty. In the case of electrical power, uncertainty in the current measurement leads to the majority of the uncertainty. The worst case is where the measured current is very low which occurs when the amount of electrical power is low or shaft speed is high causing high voltage. The large variation in uncertainty of the efficiency parameters is due to the variation already discussed in the power

parameter uncertainties. For the conditions where peak efficiency occurs in the turbines, generator, and combined turbine-generator, uncertainty tends to be closer to the best case.

For the jet velocity, jet power, and speed ratio terms, the velocity coefficient of the nozzles contributes the majority of the uncertainty. The uncertainty also propagates to the turbine efficiency term; though, velocity coefficient is not the most significant contributor there. Since the velocity coefficient is based on an assumed value (i.e. not actually measured), it is valuable to consider what impact variations in the value can have on calculated parameters such as jet velocity, jet power, turbine efficiency, and speed ratio. A large value for uncertainty of 0.01 (slightly more than 1%) for the nozzle velocity coefficient has been chosen so as to include the range of expected values suggested by Thake [24]. Table 4.3 presents the sensitivity analysis for a representative turbine efficiency test.

Table 4.3. Sensitivity analysis for nozzle velocity coefficient for a turbine efficiency test with a 169-mm Turgo turbine and an 11.11-mm nozzle. The sensitivity and percent of nominal value terms were calculated at peak turbine efficiency assuming an uncertainty value of 0.01 for velocity coefficient.

Parameter	Nominal value	Sensitivity Coefficient $(\partial R/\partial x_i)$	Local Sensitivity $\theta_i(\partial R/\partial x_i)$	Percent of nominal value
Velocity Coefficient, C_v	0.975	1	0.01	1.03%
Nozzle Efficiency, η_{noz}	0.951	1.95	0.0195	2.05%
Jet Velocity, v_j *(m/s)*	19.37	19.86858	0.198686	1.03%
Jet Power, $\dot{W}_j$ *(W)*	346	709.9235	7.099235	2.05%
Turbine Efficiency, η_t	0.867	-1.77937	-0.01779	2.05%
Speed Ratio, x	0.490	-0.50307	-0.00503	1.03%

The sensitivity coefficients represent the rate of change of each parameter for a change in velocity coefficient while local sensitivity shows the impact of the sensitivity coefficients on the uncertainty of the calculated parameter. The analysis shows about a 2% contribution to the jet power and turbine efficiency uncertainties and 1% to the speed ratio due to velocity coefficient given the assumptions made about its value and uncertainty. These uncertainties are very reasonable when compared to other parameters.

4.4 Flow Measurement Calibration

One of the largest sources of error in the power and efficiency calculations was due to the volumetric flow rate measurement. According to the manufacturer's

specifications, much of the error was due to bias. In order to minimize the bias error in the flow measurement, a calibration was conducted on the instrument. The calibration consisted of filling a container with water while measuring the total time to fill and final weight of water in the drum. Flow meter readings were taken every second for the duration of the fill, averaged over time used to generate a curve fit for the bias error. Table 4.4 shows the degree to which the uncertainty in flow rate was improved following the calibration for several flow rates.

Table 4.4. Uncertainty estimate for flow rate measurement before and after calibration.

Q, Flow Rate (gpm)	θ_Q, pre-calibration (+/- gpm)	θ_Q, post-calibration (+/- gpm)
17.426	1.0	0.143
23.048	1.0	0.173
28.254	1.0	0.281
32.431	1.0	0.403

4.5 Procedures

To ensure consistent results and safe operation, a set of procedures for set-up, startup, shutdown, and data sampling procedures were created. Flow charts have been made to aid the operator(s) during experiments.

Prior to operation, all equipment must be set-up and prepared for use. The turbine and nozzle to be used for the experiment must be installed and the nozzle aligned with the turbine visually. Once everything inside the turbine housing is installed, the panels on the sides of the housing should be inserted to ensure the water

is contained when the jet is turned on. The flow, temperature, and pressure meters are also turned on at this time. Prior to turning the pump on, it must be primed by filling the lines with water. Once priming is complete, the pump suction hose should be placed in the tank and secured so it does not move while the pump is operating. The pump is turned on by the wall switch and the ball valve can be opened to allow water to flow. The flow control valve is then used to reduce the flow and thereby reduce the shaft speed (with no load circuit connected, the alternator will spin very fast if the water flow is not reduced). Fine tuning of the nozzle position can be done by making slight adjustments and measuring shaft speed to see if it went up or down. First, the radial position of the jet should be adjusted by rotating the nozzle mount about its vertical axis. Second, the tangential position can be adjusted by moving the nozzle mount toward or away from the turbine housing. The nozzle mount system is pictured in Fig. 4.5. Once jet positioning is complete, the ball valve can be closed and pump turned off or the data sampling procedure can begin right away. The set-up/start up flow chart is shown in Fig. 4.6.

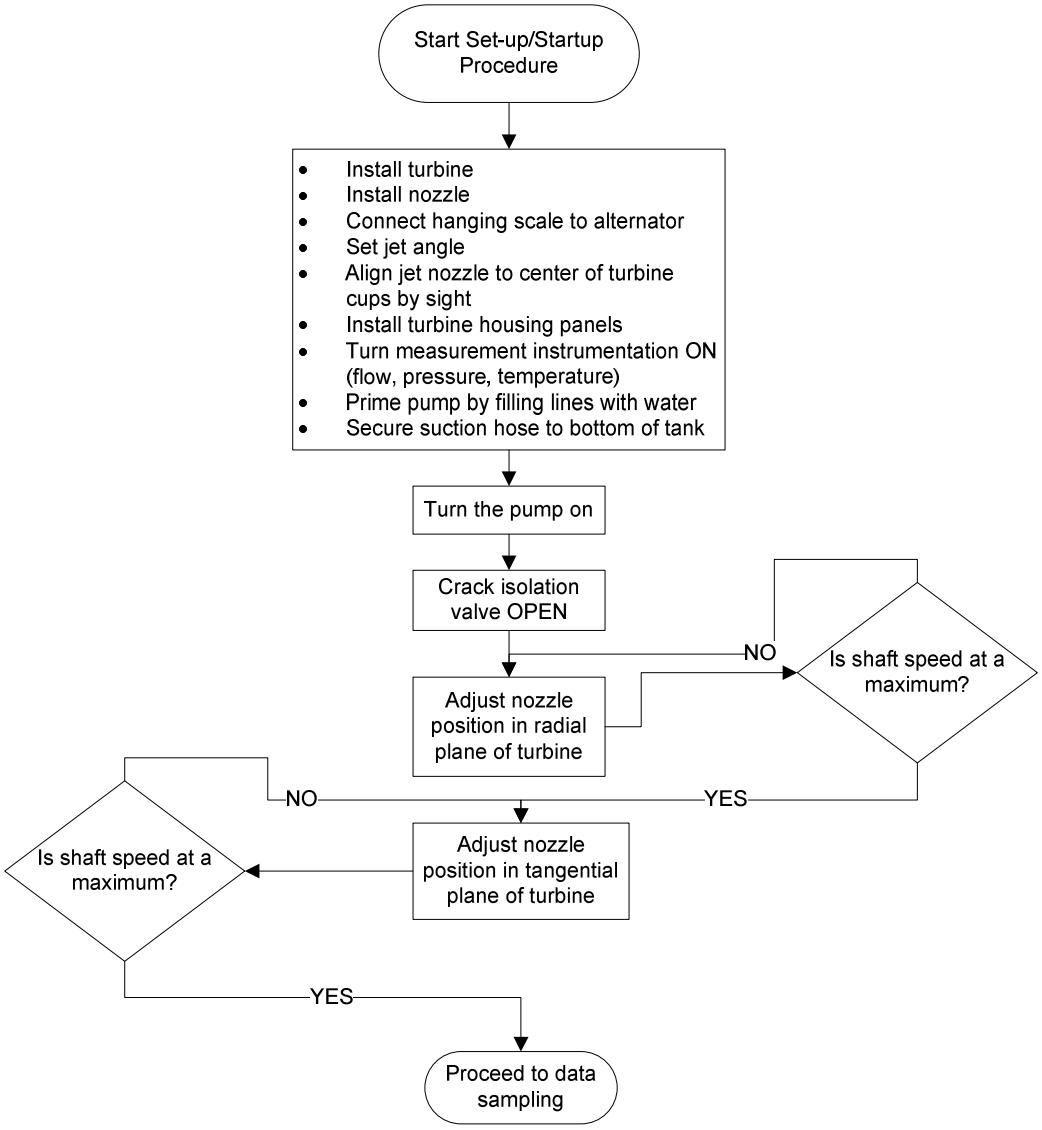

Fig.4.6. Set-up/startup procedure flow chart.

A general sampling procedures was created to accommodate all experiments; however, for certain experiments some steps can be omitted. Once set-up and startup are complete, the ball valve is shut (if not already shut) and the load circuit is configured. The circuit consisted of two 0-50 Ω rheostats and up to three light bulbs. To achieve lower speeds, the bulbs can be placed in parallel with the highest wattage

bulbs available to produce a lower resistance in the circuit. Care was taken to not exceed the 1.41 amp limit on the rheostats. The ammeter used to monitor the current flowing out of the PMA was also be used to monitor the rheostats. Higher shaft speeds were achieved by raising the circuit resistance by aligning light bulbs in series and using lower wattage bulbs. Once the circuit is aligned, the ball valve can be opened to allow water flow. The alternator and load circuit were given time to warm-up prior to data taking. If the system was at room temperature prior to starting (cold start), about 20 minutes were allowed before beginning to check for a steady voltage at the alternator terminals. When the terminal voltage had stopped changing, data was taken at approximately 50 rpm increments by adjusting the rheostat position to change shaft speed. Data points taken at this interval provide enough points for smooth plot curves. The load circuit was altered to cover the full range of shaft speeds required for a particular test. The Data Sampling Procedure flow chart is shown in Fig. 4.7.

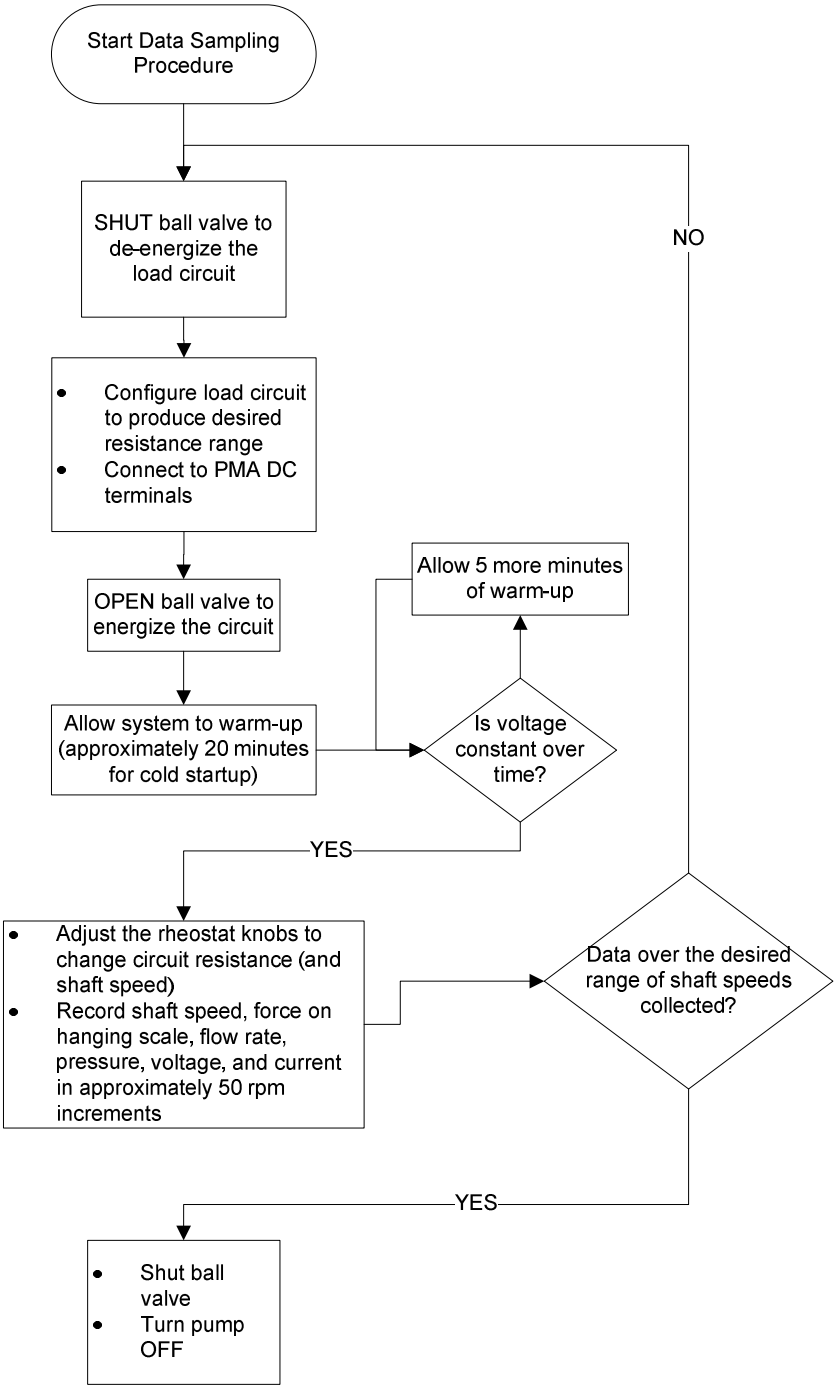

Fig. 4.7. Data sampling procedure flow chart.

The general procedure for collecting data applies to tests involving both the turbine and generator. For turbine only testing, warm-up times can be omitted since turbine performance is not significantly impacted by temperature changes in the alternator. Additionally, voltage and current do not need to be measured. When only the generator is considered, the flow rate and pressure can be left out. For flow rate and pressure measurements, a digital camera was used to record at each sampling point for approximately five seconds. Pressure changes little over the five second period and the entire data set; whereas, the flow rate fluctuates continuously. To remove the fluctuations in flow rate, five values are recorded over the five second period and averaged. Since pico-hydro operates under steady-state conditions, the five second average is justified. Sample datasheets are provided in Appendix B.

Chapter 5 – Results & Discussion

5.1 Speed Ratio

As discussed previously, turbine speed as it relates to jet velocity is an important parameter to consider, as it can have a significant impact on turbine efficiency. Speed ratio, defined in section 2.4, can be used to select the proper turbine speed given a particular jet velocity. A momentum balance, as described in section 2.6, dictates that the speed ratio should be set at 0.5, whereas, experimental studies put the actual value between about 0.46 and 0.48. Near peak efficiency, the curve is relatively flat, so the efficiency does not change much with a small change in speed ratio but losses increase more rapidly the further speed ratio deviates from the ideal value. Because turbine speed is determined prior to installation, it is valuable to be able to accurately predict the optimal speed at which the turbine should spin.

Figure 5.1 depicts how peak efficiency as a function of turbine speed shifts as jet velocity changes. As jet velocity increases, the peak shifts toward the right, to higher turbine speed. The increasing jet velocity is caused by an increase in head and causes peak turbine efficiency to occur at a higher turbine speed. Second order polynomial trendlines are used to show the shift in peak efficiency more clearly. Speed ratio can be used to nondimensionalize the turbine speed and jet velocity, resulting in the curves collapsing onto each other (Fig. 5.2). Peak efficiency occurs around a speed ratio of 0.45 in Fig. 5.2. Other tests on the two Turgo turbines used for this work showed that peak efficiency consistently fell in the speed ratio range of 0.45-0.50. Error in the jet velocity calculation and factors impacting the water velocity as it

exits the turbine such as losses resulting from flow inside the cups likely accounts for much of the deviation from the ideal speed ratio of 0.5. Speed ratios below approximately 0.45-0.46 may be the result of jet alignment problems that will be discussed later. Peak efficiency for the 169-mm Turgo turbine was measured to be over 85% for while the best efficiency for the 133-mm model was just over 81%. Compared to Pelton turbines used for the same power range, the Turgo turbines tested performed quite well. Pelton turbines in pico-hydro tend to operate in the 75-85% peak turbine efficiency range [24] while other Turgo turbines have been found to operate from 70-80% efficiency [13, 19]. Gilkes [27], a hydropower company in the UK, reports peak turbine efficiencies around 85% for their Turgo turbines ranging in power outputs from 20 kW to 10 MW).

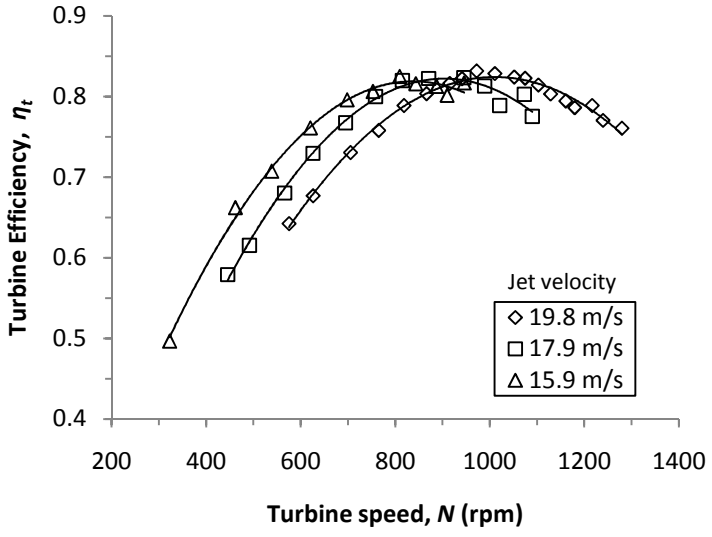

Fig. 5.1. Turbine efficiency vs. turbine speed for a 169-mm Turgo turbine with a 9.53-mm nozzle and three different jet velocities.

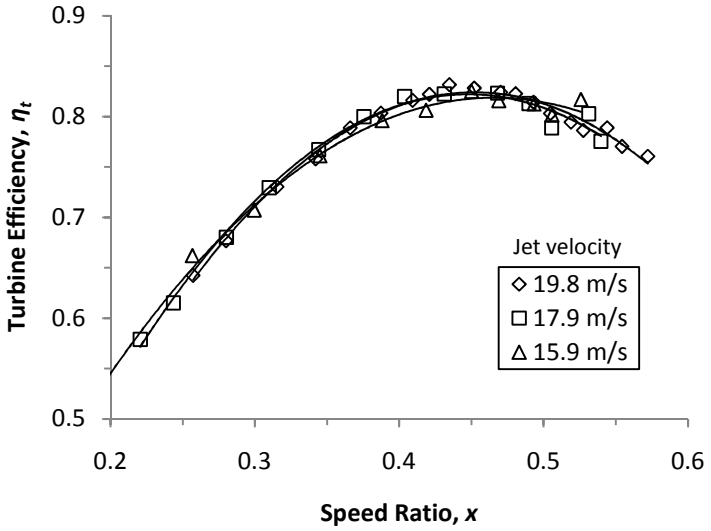

Fig. 5.2. Turbine efficiency vs. speed ratio for a 169-mm Turgo turbine with a 9.53-mm nozzle and three different jet velocities.

As expected, the Pelton turbine efficiency varies with the speed ratio just like the Turgo turbine efficiency. The same theoretical momentum balance applies resulting in the efficiency curves collapsing on top of one another when plotted against speed ratio. Figure 5.3 shows turbine efficiency vs. turbine speed for the 100-mm Pelton turbine. Once again, second-order polynomial trend lines are added to the data to clearly show that for increasing jet velocity, the turbine efficiency curve shifts toward higher turbine speeds. Figure 5.4 shows the same data plotted vs. speed ratio resulting in a common peak at a speed ratio of about 0.40-0.42. Other tests on the same Pelton turbine, using various flow and head conditions, resulted in approximately the same preferred operating point. The value for speed ratio is lower than would be expected for a Pelton turbine based on the literature [13, 24] and is

likely the result of losses due to flow disturbances within the turbine blades. A previous study found that a smooth cup surface will reduce energy losses in the turbine and increase efficiency [13]. No attempt was made to polish the Pelton turbine used for this study though doing so may improve performance by shifting the peak efficiency point toward a higher speed ratio and increasing turbine efficiency. An alternative explanation could be that the lower efficiency and shifted speed ratio results from poor jet alignment. This explanation is unlikely however, since multiple tests showed identical results (refer back to section 4.5). The highest Peak efficiency for the Pelton turbine tested here was 73%. This value is close to the peak efficiency obtained by Williams and Simpson [13], 72% for a pico-hydro Pelton turbine. For large scale hydropower, turbine efficiency is generally above 90% [24].

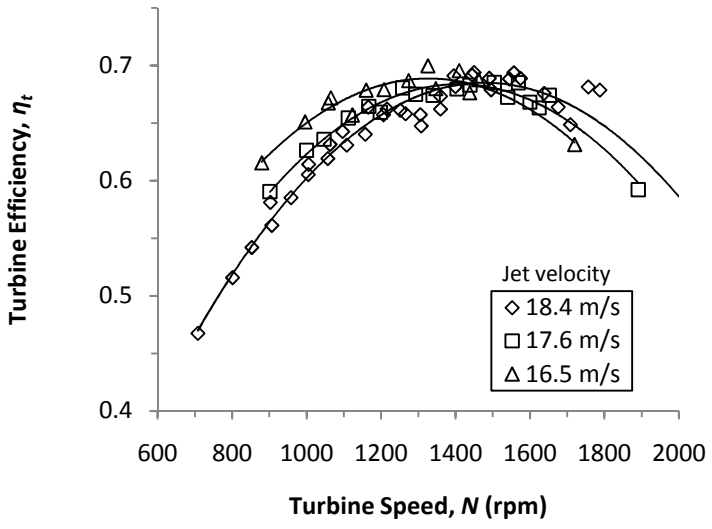

Fig. 5.3. Turbine efficiency vs. turbine speed for a 100-mm Pelton turbine with a 9.53-mm nozzle and three different jet velocities.

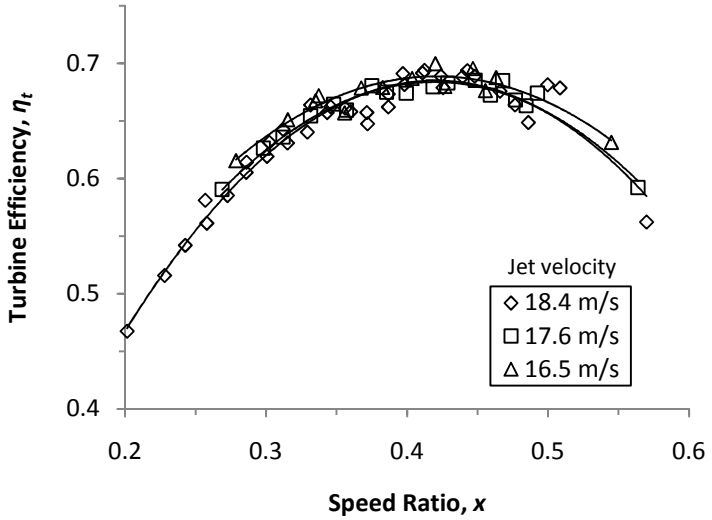

Fig. 5.4. Turbine efficiency vs. speed ratio for a 100-mm Pelton turbine with a 9.53-mm nozzle and three different jets velocities.

5.2 Misalignment

In order to achieve the desired energy transfer from the water jet to the turbine the jet must strike the turbine in the correct location. Improper jet alignment will impact the flow of the water through the turbine blades and possibly cause some of the water to miss the turbine altogether resulting in reduced turbine efficiency and lower than expected power output. A number of tests have been conducted to determine the significance of the effects of poor jet alignment.

For Pelton turbines, proper radial alignment is critical to maximizing turbine efficiency. The jet should strike the turbine blades tangent to the pitch-circle. Figure 5.5 shows what impact poor radial alignment can have. When the jet struck the turbine blades on either the inside or outside edge, efficiency dropped from over 70%

to just over 50%. Moving the jet further from the optimal radial position would result in further reduction in efficiency; however, the inside and outside edge of the blades is the worst case based on what is reasonably possible. The inside edge appears to show less of a drop in efficiency but the difference is within the margin for uncertainty, discussed in section 4.4, and should not be taken as an indication that misalignment to the inside is better than the outside. For the two poorly aligned cases in Fig. 5.5, the peak efficiency point shifts to a lower speed ratio as a result of the inefficient energy exchange.

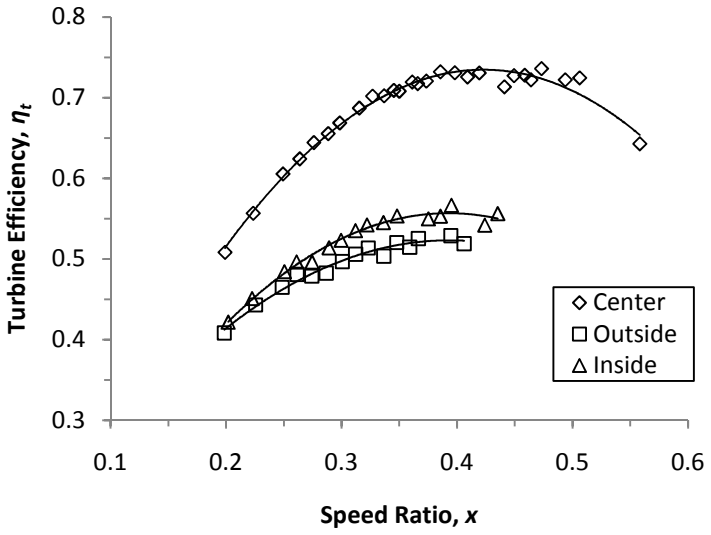

Fig. 5.5. Turbine efficiency vs. speed ratio for a 100-mm Pelton turbine with a 9.53-mm nozzle for three radial jet positions.

Figure 5.6 shows the results of angular misalignment of the jet on the same Pelton turbine. As expected, efficiency decreases as jet alignment increases. Surprisingly, a jet angle of 15° results in just a 10 percentage-point loss in efficiency.

About half of the lost power can be attributed to the jet power that is now parallel to the axis of the turbine which will not be transferred to the motion of the turbine. Angular jet misalignment of this magnitude is unlikely to occur without a major mistake by the installer but it does demonstrate a significant tolerance for angular misalignment.

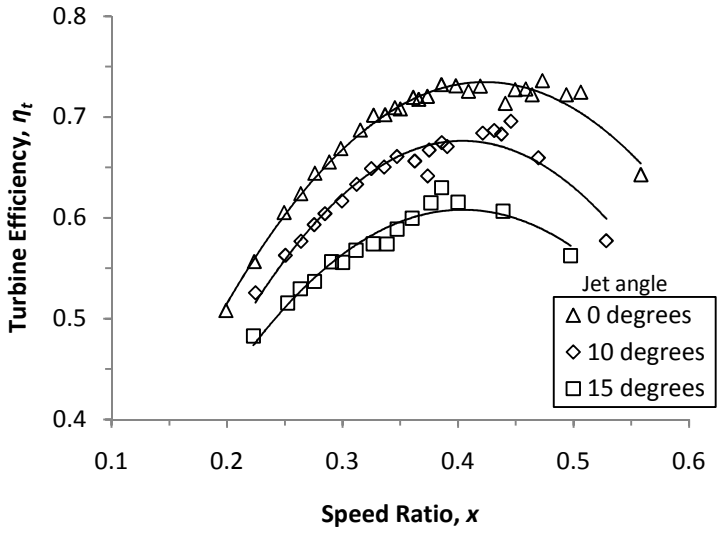

Fig. 5.6. Turbine Efficiency vs. Speed Ratio for a 100-mm Pelton turbine with a 9.53-mm nozzle for three angular jet positions

Like the Pelton turbine, the Turgo turbines can be heavily impacted by improper radial jet alignment. Figure 5.7 shows a drop in peak turbine efficiency as much as 15 percentage points for the outside misalignment and a smaller reduction for the inside. This plot also clearly shows a shift in the speed ratio at peak efficiency for both misaligned cases. The shift in speed ratio is due to effectively changing the PCD of the turbine by changing where the jet hits the turbine blades and added energy

losses in the turbine blades from the altered flow pattern. Figure 5.7 appears to show that misalignment to the inside is not as bad as the outside, similar to Fig. 5.6. For misalignment to the outside, it may be more likely that water from the jet will miss the turbine altogether; however, the most important point to take is that a modest radial misalignment can have a noticeable negative impact on turbine performance by reducing the peak efficiency and shifting the speed ratio at peak efficiency.

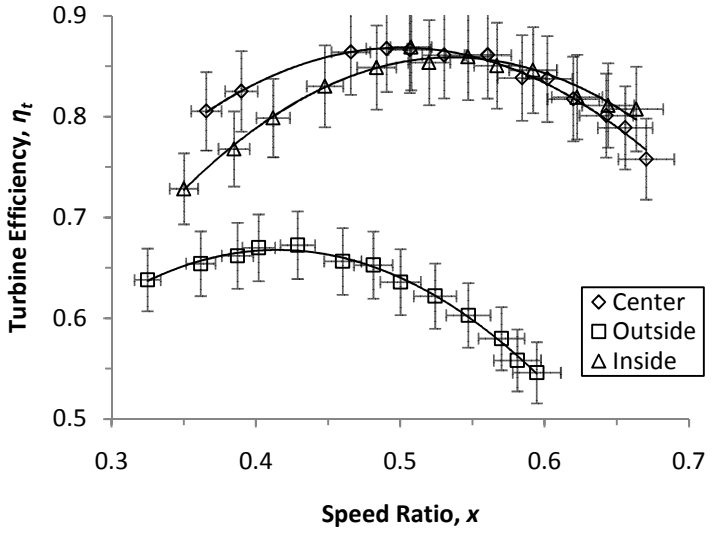

Fig. 5.7. Turbine efficiency vs. speed ratio for a 169-mm Turgo turbine with an 11.11-mm nozzle for three radial jet positions. Error bars are shown for speed ratio (horizontal) and turbine efficiency (vertical).

Angular misalignment is more of a concern for Turgo turbines than it is for Pelton turbines for the simple reason that the installed jet angle is not intended to be zero. Figure 5.8 shows how much of an impact the jet angle has on Turgo turbine efficiency. Reducing the jet angle from 20° to 18° appears to reduce efficiency by a

little less than 5 percentage points, though some of this reduction could result from the repeatability of the experiment. Repeated tests showed that both 18° and 20° jet angles produced peak turbine efficiencies of approximately 85%. A more significant drop in efficiency is observed for 14° and 24° jet angles, with close to a 10 percentage-point reduction. For the jet angle above 20°, peak efficiency appears to shift to the right toward a higher speed ratio. It may be possible that the jet strikes the turbine closer to the inside of the blades for the 24° test, resulting in a smaller effective PCD.

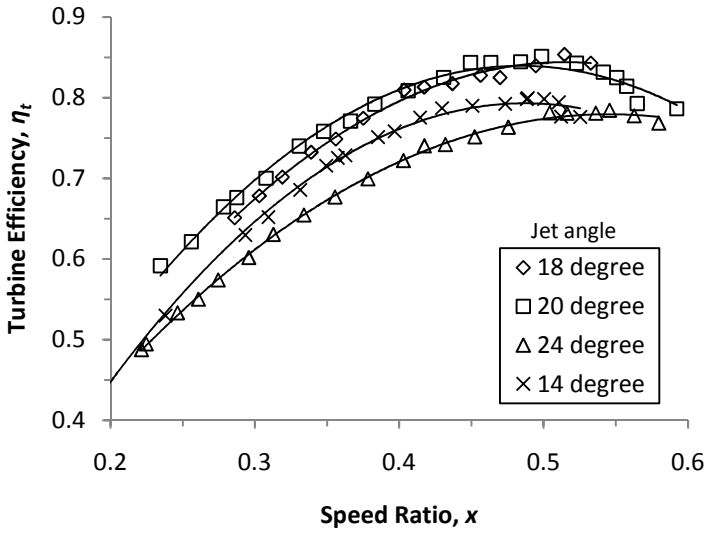

Fig. 5.8. Turbine Efficiency vs. Speed Ratio for a 169-mm Turgo turbine with a 7.94-mm nozzle for four angular jet positions.

5.3 Jet Quality

Figures 5.9 and 5.10 show what impact a poorly constructed nozzle and manifold can have on jet quality. The jet in Fig. 5.9 is much smoother than the jet in

Fig. 5.10. A well designed rounded nozzle was used for the first jet compared to the homemade plastic nozzle made by drilling a hole in a plug placed at the end of a pipe, essentially a sharp edged orifice. Proper nozzle design allows for a smooth reduction in cross-sectional area from pipe to the jet resulting in less of the kinetic energy of the flow being lost to secondary flow structures and a less divergent jet. For the homemade nozzle (Fig. 5.10), the jet begins to diverge immediately, has a non-uniform cross-section, and has a much rougher surface. The roughness and early divergence in the jet are caused by secondary flow structures in the jet that give the water momentum in the radial plane. Energy transfer to the turbine will be reduced due to some water missing the turbine altogether and reduced mean jet velocity of (i.e. lower kinetic energy in the direction of the jet). Based on the head loss calculations discussed in section 2.4, as much as a 10-m head loss can be expected in the plastic nozzle compared to about 1 m for the brass nozzle. Since the jet head was not measured directly in this study, the head loss in the nozzles cannot be verified. Nonetheless, the results clearly indicate that the nozzles, which are important for producing a high-quality jet, can have a significant impact on energy transfer from the water to the turbine.

Fig. 5.9. A good-quality jet from a well-made machined brass nozzle.

Fig. 5.10. A poor-quality jet from a homemade plastic nozzle.

Figure 5.11 shows the difference in efficiency that jet quality can have on a Pelton turbine. The plot shows about a 10 percentage-point drop in efficiency for the lower quality jet to the right of the plot where the curve from the plastic nozzle terminates. Due to the poor energy transfer from the jet to the turbine, the turbine could not be rotated fast enough to reach a peak turbine efficiency. A larger load resistance would be necessary to achieve the higher speed. Had a peak been reached, it most likely would have been shifted toward the left of the graph due to more energy losses in the turbine arising from less uniform water flow through the turbine cups. For the efficiency test, every attempt was made to line up both jets where the most

efficient energy transfer took place. In the case of the plastic nozzle, efficiency would have been nearly zero had alignment not been adjusted to account for the non-uniformity in the jet.

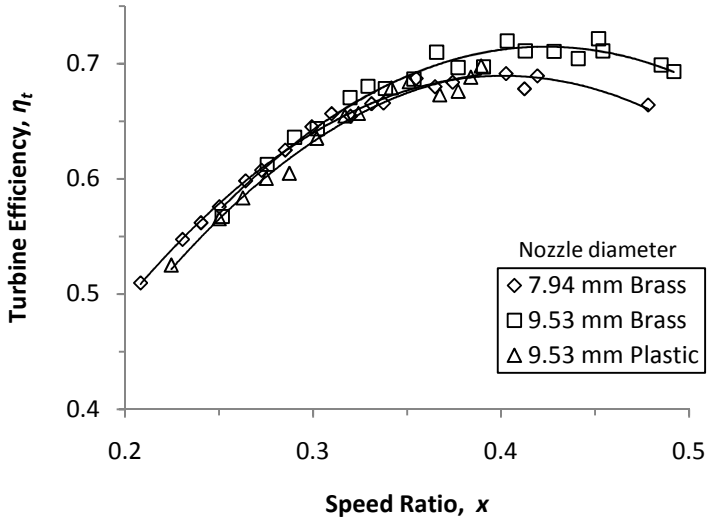

Fig. 5.11. Turbine efficiency vs. speed ratio for a 100-mm Pelton turbine with smooth and rough jets.

5.4 Scaling

To verify that results from this research would be applicable to flow and head conditions outside of those tested, the impact of changes in head, specific speed, and flow rate were investigated for both Pelton and Turgo turbines. Installed pico-hydro systems may utilize heads up to about 100-200 m [24]. For medium head applications, where Turgo turbines are most likely to be used, head is below 50 m [23]. The system used in this study is capable of producing heads up to about 30 m. For the lower power applications encounter with pico-hydro, the impulse turbines used

are generally not so large that they need to be scaled down, so little consideration was given to changes in turbine size. Figure 5.12 shows typical head and flow rate ranges for different size Pelton turbines. As Fig. 5.12 shows, a 200-mm Pelton turbine should be capable of accommodating most flow and head conditions up to about 5 kW.

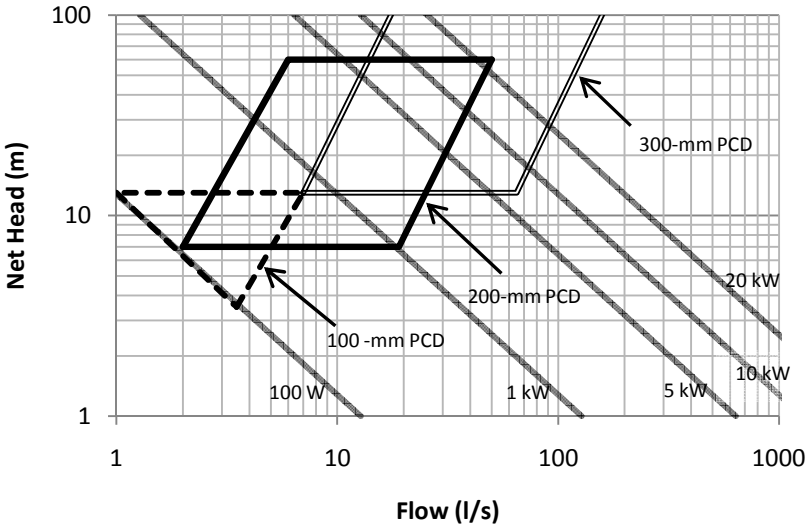

Fig. 5.12. Pelton turbine application ranges for 100, 200, and 300-mm PCD (adapted from Thanke [24]).

Figure 5.13 shows turbine efficiency vs. speed ratio for a Turgo turbine with a constant nozzle diameter but a variable hydraulic head. The plot shows effectively no difference in efficiency from one head to another. Peak efficiency for each test was over 80% efficiency and a speed ratio of about 0.45. It is worth noting that as head changes the specific speed remains nearly constant as long as the nozzle diameter does not change as Fig. 5.14 shows. In Fig. 5.14, all four curves are once again nearly indistinguishable from one another. The two plots indicate that a change in head should not have much of an impact on turbine efficiency at least for the case where

specific speed does not change significantly. A change in head with little or no change in specific speed can be achieved by varying the head while keeping the nozzle diameter constant. For practical applications, this result suggests that for a particular nozzle size, turbine efficiency of a Turgo turbine will not change significantly for a change in head over the range tested here, 13-28 m. The head range from 13-28 m is significant since it includes the most applicable range for Turgo turbines [27]. Similar plots can be generated for Pelton turbines as shown in Fig. 5.15 and 5.16 with the same result seen in the Turgo turbine data.

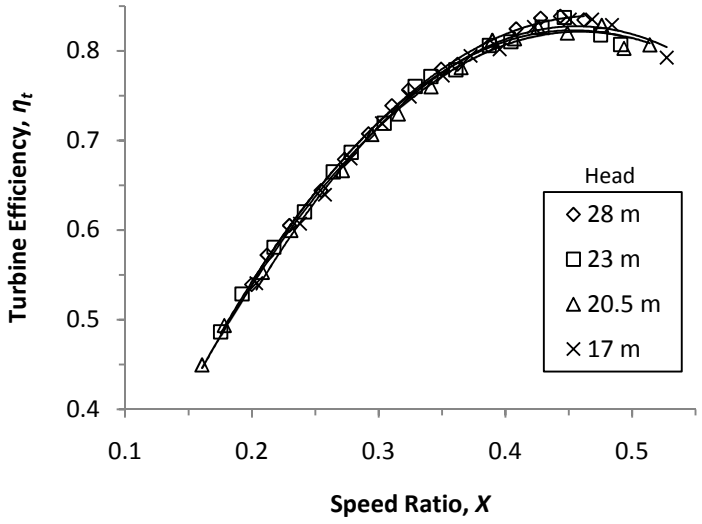

Fig 5.13. Turbine efficiency vs. speed ratio for a 169-mm Turgo turbine with a 7.94-mm nozzle for various values of head.

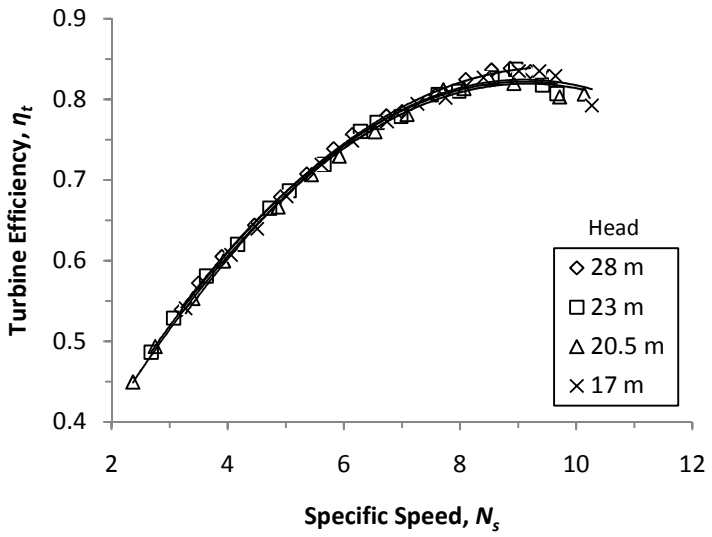

Fig. 5.14. Turbine Efficiency vs. Specific Speed for a 7.94-mm nozzle and a 169-mm PCD Turgo turbine for various values of head.

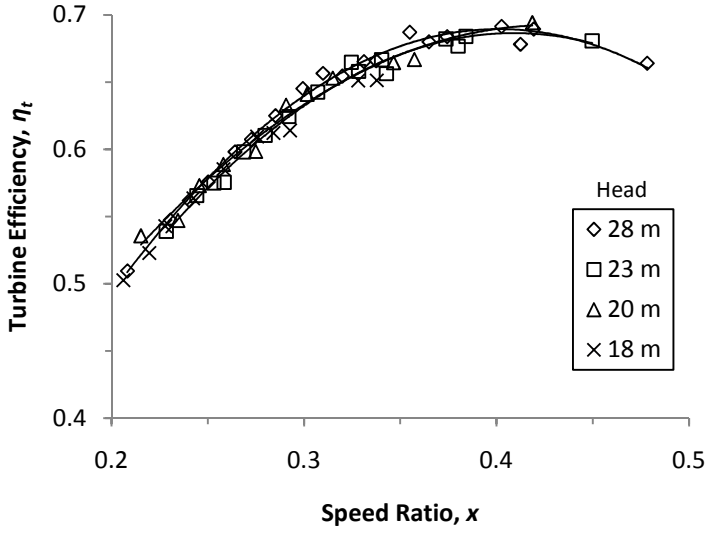

Fig. 5.15 Turbine efficiency vs. speed ratio for a 100-mm Pelton turbine with a 7.94-m nozzle for various values of head.

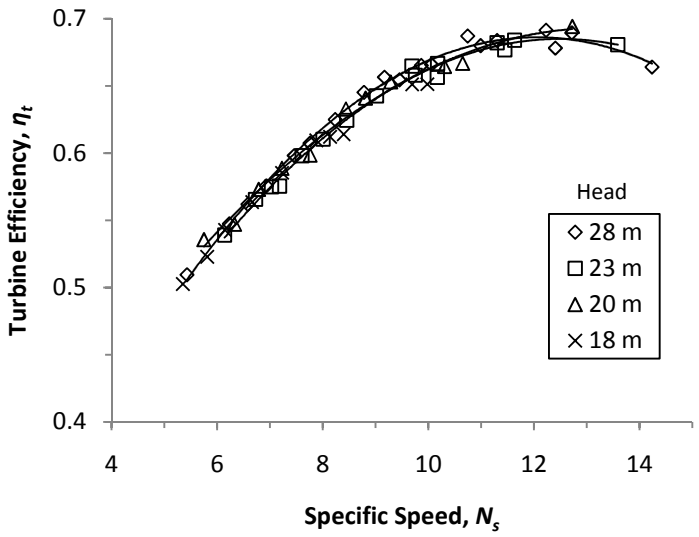

Fig. 5.16 Turbine efficiency vs. specific speed for a 100-mm Pelton turbine with a 7.94-mm nozzle for various values of head.

In Fig 5.17, several different values of head were used; this time however, the change in head was accomplished by a change in nozzle diameter. Since a centrifugal pump was driving the flow in the experimental set-up, a change in nozzle size resulted in a higher flow rate and lower head due to a change in pump efficiency corresponding to the pump performance curve (see Appendix A). Like in Fig. 5.13, no change in turbine efficiency is observed for a change in head. Figure 5.18 shows the same turbine efficiency data as a function of specific speed, showing a clear change in specific speed due to the difference in head and flow rate. The data show that even when specific speed is not held constant, changes in head have no noticeable impact on peak efficiency for Turgo turbines. It is likely that under more extreme operating conditions, such as very low or high head, other factors such as bearing or windage losses will have a significant impact and cause changes in efficiency. For medium

head, between 10 and 50 m, these other factors should not have a major influence on turbine performance. Another likely important consideration is nozzle size. No guidelines for maximum nozzle diameter for a particular turbine are widely available, though above some point turbine efficiency will most certainly be negatively impacted. For this study, the maximum nozzle diameter used was 1/2" corresponding to roughly 10% of PCD and 33% of the cup width no apparent impact on turbine efficiency.

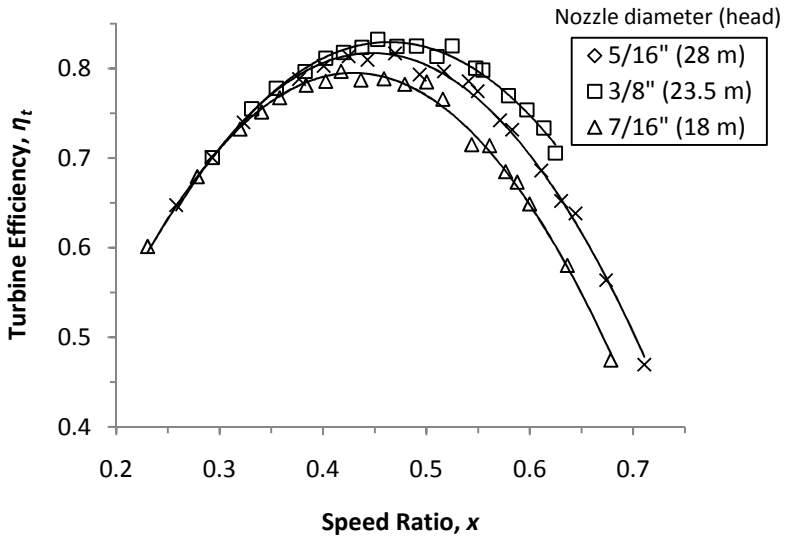

Fig. 5.17 Turbine efficiency vs. speed ratio for 131-mm Turgo turbine for various values of head and nozzle size.

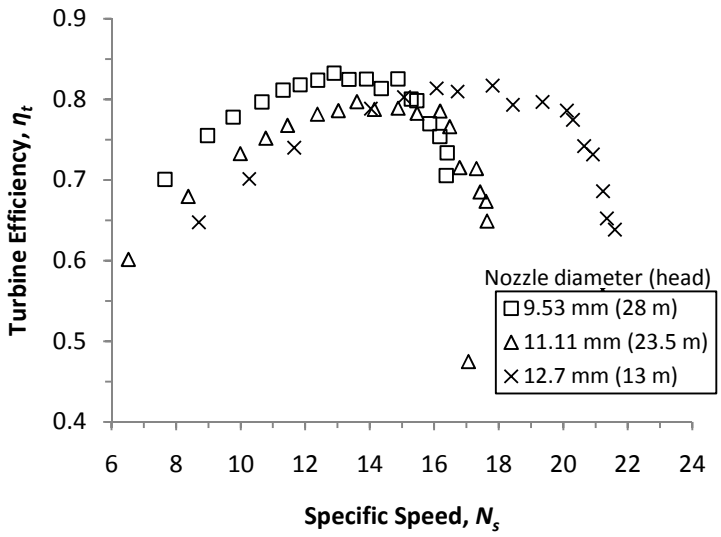

Fig. 5.18 Turbine efficiency vs. specific speed for a 131-mm Turgo turbine for various values of head and nozzle size.

Similarly, the Pelton turbine efficiency shows no signs of changing appreciably for changes in head and nozzle size within the achievable range (Fig. 5.19). The specific speed is also shifting for the three cases of head and nozzle size presented for the Pelton turbine (Fig. 5.20). Published guidelines do exist for sizing nozzles to maximize Pelton turbine efficiency [24]; it has been suggested that a maximum nozzle size of approximately 11% of PCD be used for Pelton turbines. If greater flow rates are required than will be allowed by this nozzle size, additional jets can be added or a larger turbine is recommended. Another investigation into maximum nozzle size found that when maximizing the power output to cost ratio, a maximum nozzle diameter closer to 17% may be advised [13]. Though efficiency begins to drop appreciably above the 11% limit, the higher flow rate raises the power output faster

than efficiency lowers it, up to a nozzle diameter of 17% of PCD. Provided the water flow rate can be raised with no added cost, the unit cost of power ($/kW) will be reduced up to the higher limit.

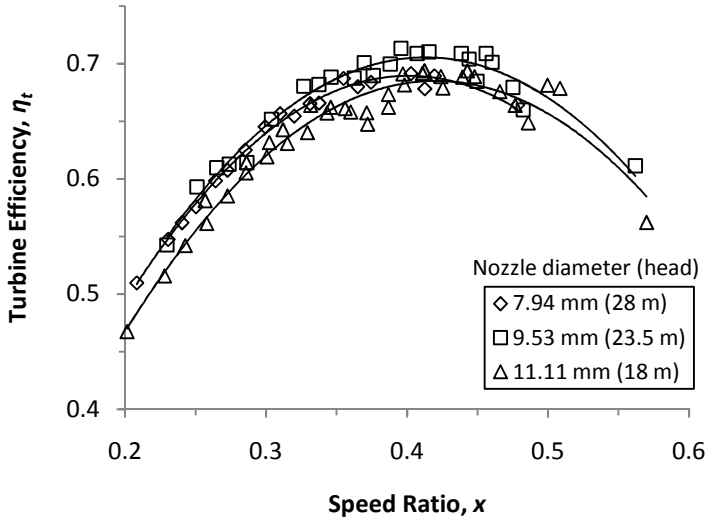

Fig. 5.19. Turbine efficiency vs. speed ratio for a 100-mm Pelton turbine for various values of head and nozzle size.

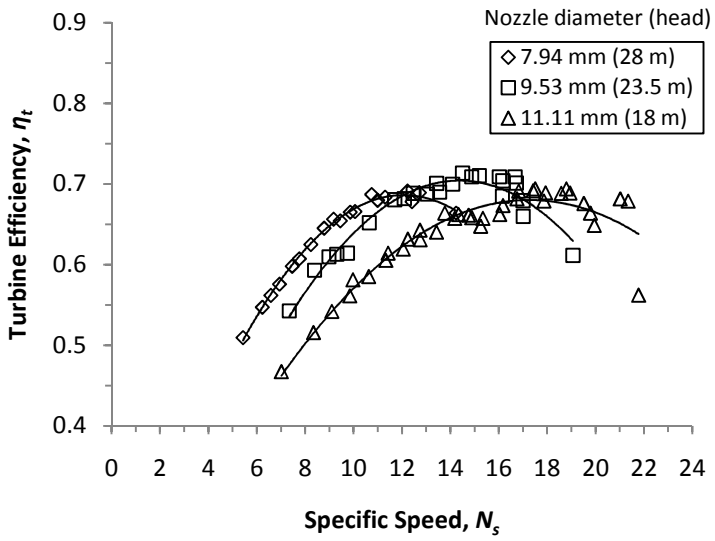

Fig. 5.20. Turbine efficiency vs. specific speed for a 100-mm Pelton turbine for various values of head and nozzle size.

Two different sizes of Turgo turbine were used for testing, a 133-mm and a 169-mm PCD turbine. Identical cups were used on the two turbines though the larger one had 28 compared to the other's 20. It is difficult to draw conclusions as to the extent PCD has on turbine efficiency for Turgo turbines since only two sizes were used, though the data shows the larger of the two Turgo turbines consistently operated at a higher efficiency. It is possible that the larger turbine provides more room for error with jet alignment. A more likely answer is that the larger PCD allowed for a better transfer of energy because of cup orientation, position or greater number of cups.

From the literature, it is clear that changes in flow rate with relatively constant head and jet diameter have little impact on turbine efficiency over a wide range. Figure 2.7 shows turbine efficiency vs. proportion of rated flow for various turbine

types. The curve for Pelton turbines, which is also applicable to Turgo turbines [14], shows that turbine efficiency varies only a few percentage points from about 0.20-1.00 of rated flow. For the purpose of pico-hydro, such a small change is insignificant.

The data presented show that for heads from about 13 m up to 30 m, for the range of specific speeds presented here, and nozzles up to at least 12.7 mm, peak turbine efficiency is impacted little by changes in flow and head. For this study, the specific speeds for tests done in this study fell in the range of 10-20. To produce 5 kW at 30 m of head, the specific speed would be closer to 50. An increase in head will result in a higher jet velocity which is not expected to impact efficiency provided the proper speed ratio is used. As for nozzle diameter, the results of this study show that ½" is not too large for the Turgo turbines used but do not indicate how much larger the nozzle could be. The results presented in this study should then be applicable to higher power applications over a similar range of specific speeds for both Turgo and Pelton turbines. A slightly larger variation in the efficiency curves from one condition to another is apparent in the plots where nozzle size was changed though no trend is present. The shift can be attributed to having to readjust the nozzle position following the nozzle change.

5.5 Generator Efficiency

Generator efficiency for a permanent magnet alternator (PMA), such as the DC-540 (Windblue Power, New Strawn, KS) depends mainly on generator power and shaft speed. For a particular amount of power, there is an optimal speed at which to

operate. The speed will depend on the alternator design and the sources of power loss within the alternator. In this study, a series of experiments were conducted to characterize how the generator efficiency of the DC-540 PMA varies with changes in power and shaft speed.

Figure 5.21 shows generator efficiency vs. electrical power for several shaft speeds. Both data provided by the manufacturer (490, 650, 870, and 1160 rpm) and those were gathered through this experiments are plotted on the same graph. As shaft speed increases, the electrical power at which efficiency peaks shifts further to the right of the graph. This shift indicates that for a particular PMA, shaft speed should increase as the power generated increases. The change in efficiency of the PMA as shaft speed and electrical power change can be explained by impedance matching (i.e. the generator operates most efficiently when the resistance of the load circuit matches the impedance of the armature windings of the PMA)[88]. This matching can be done by adjusting the resistance in the load circuit, thereby changing the voltage, current and shaft speed. The data provided by the manufacturer for the DC-540 PMA indicates a lower efficiency than the data generated in this work. An error in the generator efficiency from this study could be caused by measuring higher than actual electrical power or lower than actual mechanical power. Electrical power can be measured with a high degree of confidence using digital multi-meters as was the case here making that an unlikely source of error. There is less confidence in the mechanical power measurement into the PMA; however, for actual mechanical power to be higher than what has been measured, either turbine efficiency or jet power would

need to be higher than calculated. Peak efficiency for the Turgo turbines has been found to be near 85% (already a very high value for pico-hydro) and the jet power measurement, which is primarily influenced by the pipe pressure measured by a pressure transducer, is expected to be accurate. The more likely scenario is that the testing procedures differed in the amount of time allowed for the PMA to heat up. Properties of the magnet and stator windings are influenced by temperature effects and significant changes in temperature do occur in the PMA when in operation [89]. Further investigation is required to show that the temperature effect is responsible for the change in performance. Nonetheless, the trend of alternator efficiency varying with shaft speed and power is clearly shown in both data sets. Also important to note, as shaft speed and electrical power increase, the efficiency curve flattens out leading to less variation over a wider range.

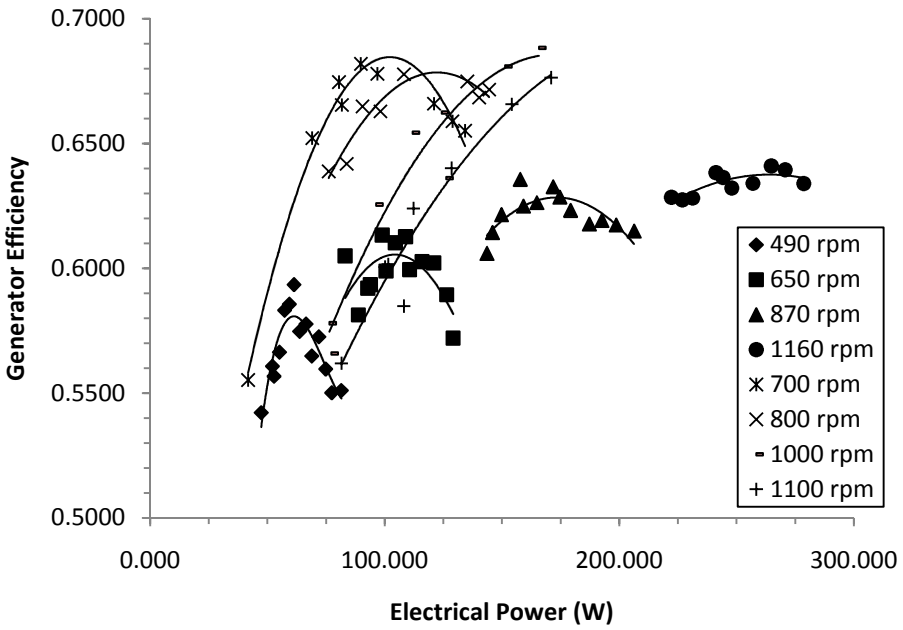

Fig. 5.21 Generator efficiency vs. electrical power for a DC-540 PMA at various shaft speeds.

If AC power is the desired output of the alternator, the frequency of the output must also be properly controlled. The electrical frequency is determined by the number of poles in the alternator and the shaft speed. A four pole alternator for example must operate at 1800 rpm in order to get a frequency of 60 Hz. To achieve a reasonable efficiency and a particular electrical frequency, an alternator must be selected that closely matches the expected power. Voltage can easily be modified by installing transformers in the load circuit but a PMA that produces power at the desired voltage and frequency at the same speed is the better option. Unfortunately, retailers in the US often do not provided information on power rating and efficiency making it difficult to correctly size PMAs.

5.6 Turbine-Generator Efficiency

Figure 5.22 shows turbine, generator and combined turbine-generator efficiency vs. shaft speed. The plot clearly shows a dependence on shaft speed. For the turbine, efficiency goes up as the shaft speed changes such that the operating condition approaches the preferred speed ratio. The generator curve is slightly more complicated. As discussed earlier in section 5.5, the PMA has an ideal speed at which to rotate for a particular power. To the left of the peak generator efficiency, the increasing shaft speed takes the generator closer to its preferred speed for the amount of power being put into the generator. This increase in efficiency, however, is somewhat mitigated by rising power caused by improved turbine efficiency. This second effect flattens out the generator efficiency curve. To the right of the peak generator efficiency, these two effects are still at work; this time both are working to reduce efficiency, resulting in a steeper curve.

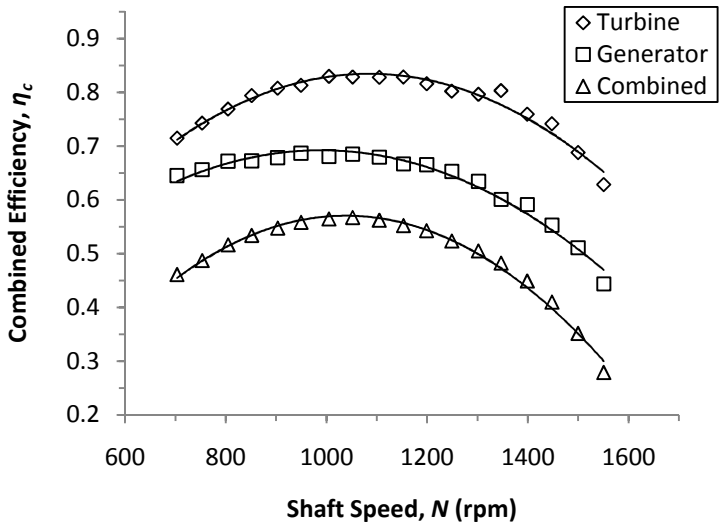

Fig. 5.22. Combined turbine-generator efficiency vs. shaft speed for a 169-mm Turgo turbine and DC-540 PMA with good turbine-generator matching.

In Fig. 5.22, peak efficiency for both the turbine and generator occur at nearly the same speed. The result is higher peak efficiency for the combined turbine-generator efficiency. Figure 5.23 on the other hand shows a turbine and generator that are not well matched. The efficiency curves peak at different speeds, the generator at about 800 rpm and the turbine near 1400 rpm. The shift resulted in a drop on efficiency from over 55% to less than 50%. Having the two curves out of phase results in lower combined peak efficiency since neither the turbine nor the generator will be operating at or near its best efficiency point when the combined efficiency peaks. Peak combined efficiency in Fig. 5.23 is about 48.4%, 5.4 percentage points lower than if the two curves had peaked at the same point.

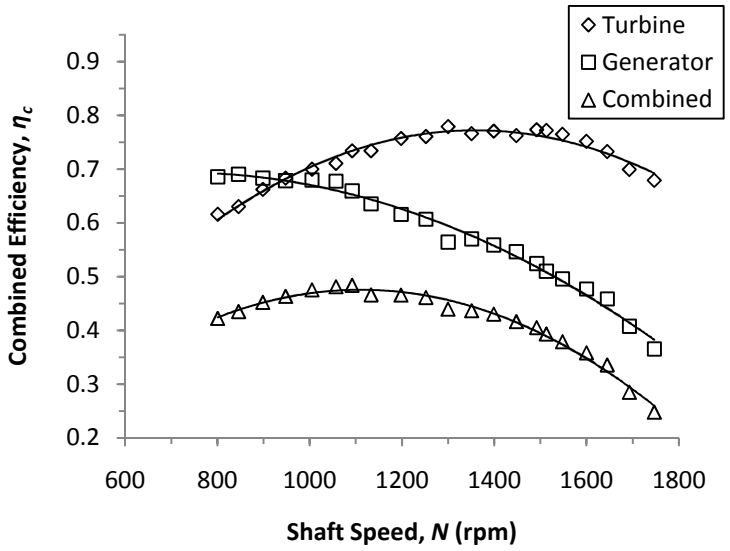

Fig. 5.23. Turbine-generator efficiency vs. shaft speed for a 169-mm Turgo turbine and a DC-540 PMA with poor turbine-generator matching.

These results illustrate the importance of selecting the right combination of turbine and generator when dealing with PMAs for pico-hydro. The two examples provided showed that a significant reduction in combined efficiency can result from poor turbine-generator matching. Knowing the preferred speed of the PMA for a given mechanical power input would be very useful for selecting the proper generator for a particular application. The turbine could be selected based on the desired shaft speed and jet velocity in order to maximize system efficiency. If the intent is to generate standard frequency and voltage electricity with the PMA, a generator with a power rating near the expected power output must be selected to avoid a reduction in efficiency caused by the power/speed mismatch.

Chapter 6 – Summary & Conclusion

Pico-hydropower is a viable technology for rural electrification in some of the most distant, impoverished regions of the world. Where suitable sites can be found, with adequate and consistent water resources, pico-hydro should be the first option considered for off-grid electrification. Provided adequate consideration is given to site-specific conditions and installation [15], pico-hydro is likely to be the most economical solution. As shown by the experiments in this study, proper equipment selection and installation are key components to achieving reasonable system efficiencies, and thereby raise power output. As Williams and Simpson [13] have shown, raising system output without added costs will reduce the unit cost of electricity ($/kW).

For impulse turbines, proper speed ratios are essential for efficiency energy transfer from the water jet to the generator shaft. Theoretically, the Pelton turbine efficiency peak will occur at a speed ratio of $x=0.5$. However, as the analysis in section 2.6 shows, the theoretical peak efficiency point for the Turgo turbine happens at approximately $x=0.53$ for a jet angle of 20°. In reality, peak efficiency occurs at a lower speed ratio for both turbine types, but the 0.03 shift remains evident. A second consideration pertaining to speed ratio that must be considered is the shift in peak efficiency due to low turbine efficiency. The further the turbines' maximum efficiency deviates from the ideal conditions, the lower the optimal speed ratio becomes. Correctly accounting for the shift in speed ratio can prevent a 5-10% loss in turbine efficiency. The effect that the speed ratio can have on turbine efficiency also

means it is important to accurately determine the net head prior to installation, since it is required for determining jet velocity.

Proper jet alignment is another essential component to consider. Even small misalignments (a few centimeters or degrees) can have significant negative effects on turbine efficiency. While angular misalignment of the jet for Pelton turbines had a fairly small impact (only about 5% for a 10° misalignment), the radial misalignment was quite a bit worse (closer to 15-20% for half a cup width). Care must be taken in the installation process to make certain the jet strikes the turbine in such a way that an efficient transfer of energy can occur. Results from this study demonstrate that visual adjustments are not adequate for achieving the highest turbine efficiency. A standardized turbine housing with built in nozzle mounts would simplify alignment. The housing would need to allow for large scale adjustments to accommodate different turbine sizes, as well as for fine adjustments to optimize the position during testing.

Jet quality can also have considerable impact on turbine performance. For the pico-hydro scale, perfect jets are not essential; however, divergence, non-uniformity and jet roughness can have an impact. Well-made nozzles are the most important component to ensure that a jet is smooth enough for pico-hydro. The machined brass nozzles used in this study produced fairly smooth jets that performed well enough that reasonable turbine efficiencies were obtained. The homemade plastic nozzle added significantly to head loss and produced a rough jet that lead to lower turbine

efficiency, approximately 10-15 percentage points less than the brass nozzles. Accordingly, this study clearly demonstrates that good quality nozzles are worth the added short-term expense. To a lesser extent, bends, pipe fittings, and contractions in the penstock and manifold can also contribute to secondary flow structures in the water that can have negative effects on the jet. Efforts should be made to minimize these types of flow disturbances but nozzle selection is much more important for jet quality.

Since not all flow and head conditions that exist for pico-hydro could be simulated using the laboratory test fixture, it is helpful to consider how different conditions will impact turbine performance. The data presented in this study show that changes in head, flow rate, and specific speed have little if any impact on turbine efficiency over the ranges tested. Previous studies support this finding with the added caveat that the jet diameter must not be too large for the turbine to accommodate. For the Pelton turbine, the limit at which efficiency begins to drop appreciably is approximately 11% PCD. No such limit has been established for Turgo turbines, although it is known to be less restrictive than the limit for the Pelton turbine. With this limitation on jet diameter in mind, the turbine performance results in this study are applicable within the pico-hydro range.

PMA efficiency is clearly related to the power output and shaft speed. For a particular shaft speed, there is a particular power output (or input) at which the generator efficiency peaks. Additionally, as shaft speed increases, the power

corresponding to peak efficiency increases and the efficiency curve flattens. The relationship between shaft speed, power output and turbine efficiency is explained by impedance matching. For practical applications with pico-hydro, generator performance data on PMAs would be extremely useful. With AC power generation, shaft speed will be dictated by voltage and frequency requirements; therefore it is important to know the rated power of the PMA as well as the percentage of rated power that it must run at to operate efficiently. When DC power is the desired output (e.g. battery charging), shaft speed is not dictated by frequency and voltage requirements and can thus be chosen such that efficiency is maximized.

Both PMAs and impulse turbine efficiencies vary with rotational speed. When selecting a PMA and turbine that will work together care must be taken to match the speeds of both components. If shaft speed of the PMA is dictated by other requirements (e.g. voltage and frequency), then a turbine must be chosen that can work efficiently at the same speed. The turbine PCD can be selected to match the PMA, or the turbine can be connected to the PMA by a gear or pulley.

There are several areas for future work on this project that have the potential to improve pico-hydro. The flow limitations for Turgo turbines need to be established in relation to PCD and/or cup size (similar to the way it has been established for Pelton turbines). A Turgo turbine and turbine-generator set should also be designed that can be built using basic manufacturing techniques. Most importantly, a general awareness and technical understanding of successful pico-hydro technology needs to be

developed and fostered at the local and regional levels so that rural electrification projects can be implemented effectively.

Bibliography

[1] Asian Development Bank. Energy outlook for asia and the pacific, Mandaluyong City, Philippines, 2009.

[2] United Nations Development Programme (UNDP), UNDP and energy access for the poor: energizing the millenium development goals, 2010, Available from: www.undp.org/energy [accessed 08.02.2011]

[3] J. Saghir, Energy and poverty: myths, links, and policy issues, Energy and Mining Sector Board, World Bank, 2005, Available from: http://siteresources.worldbank.org/INTENERGY/Resources/EnergyWorkingNotes_4.pdf [accessed 06.27.2011]

[4] European Small Hydropower Association. Small hydropower for developing countries, 2005, Available from: http://www.esha.be/fileadmin/esha_files/documents/publications/publications/Brochure_SHP_for_Developing_Countries.pdf [accessed 08.02.2011]

[5] M. Gnecco, Mechanical refrigeration using Pelton turbines, in: Pico Hydro News, Nottingham Trent University, Nottingham, UK, 1997, pp. 5-6.

[6] N. Smith, P. Maher, A. Williams, Pico hydro for cost-effective lighting, in: Boiling Point Magazine, 2007.

[7] H.P. Bjørnåvold, A feasibility study on the implementation of a micro-hydro scheme in Sioma, Zambia, University of Warwick, School of Engineering, 2009, Available from: http://www.ewb-uk.org/system/files/Hans+Petter+Bjornavold+report.pdf [accessed 08.02.2011]

[8] United Nations (UN). 2009-2010 annual performance report of UNDP supported GEF financed projects, in, UN Development Programme, New York, NY, 2011, pp. 33.

[9] Illustrated guide to financing micro hydro, Available from: http://practicalaction.org/micro-hydro-power-3 [accessed 06.27.2011]

[10] L. Wang, D.J. Lee, L.Y. Chen, J.Y. Yu, S.R. Jan, S.J. Chen, W.J. Lee, M.H. Tsai, W.T. Lin, Y.C. Li, A micro hydro power generation system for sustainable microgrid development in rural electrification of Africa, in: IEEE Power Energy Society General Meeting, Calgary, Canada, July 20-24, 2009, pp. 1-8.

[11] World Bank Energy Unit. Technical and economic assessment of off-grid, mini-grid, and grid electrification technologies annexes, 2006, Available from:

http://energyaccess.wikispaces.com/file/view/WBElectrificationAssessment17May07.pdf [accessed 08.02.2011]

[12] P. Maher, N. Smith, A. Williams, Assessment of pico hydro as an option for off-grid electrification in Kenya, J Renew Energy, 28 (2003) 1357-1369.

[13] A. Williams, R. Simpson, Pico hydro-Reducing technical risks for rural electrification, J Renew Energy, 34 (2009) 1986-1991.

[14] A. Harvey, A. Brown, P. Hettiarachi, A. Inversin, Micro-hydro design manual: A guide to small-scale water power schemes, Practical Action Publishing, Warwickshire, UK, 1993.

[15] J. Holderman, 2011, Little Green Baby Steps: Transforming Modern Power Production through Microscale Hydropower, thesis (Master of Science), Oregon State University

[16] K. Alexander, E. Giddens, Microhydro: Cost-effective, modular systems for low heads, J Renew Energy, 33 (2008) 1379-1391.

[17] World Bank, Directions in hydropower, 2009, Available from: http://siteresources.worldbank.org/INTWAT/Resources/Directions_in_Hydropower_FINAL.pdf [accessed 08.02.2011]

[18] Energy Systems & Design, Available from: http://www.microhydropower.com/index.htm [accessed 07.19.2011]

[19] P. Cunningham <hydropow@nbnet.nb.ca>, Engergy Systems & Design, personal communication [sent 7.27.2011]

[20] NoOutage.com, Available from: www.nooutage.com [accessed 07.18.2011]

[21] Home Power, Available from: www.homepower.ca [accessed 07.20.2011]

[22] K. Sopian, J. Razak, Pico Hydro: clean power from small streams, in: WSEAS Renew Energy Sources, Lalaguna, Spain, July 1-3, 2009, pp. 414-419.

[23] O. Paish, Small hydro power: technology and current status, Renew Sustain Energy Rev, 6 (2002) 537-556.

[24] J. Thake, The micro-hydro Pelton turbine manual: design, manufacture and installation for small-scale hydro-power, ITDG publishing, 2000.

[25] P. Maher, N. Smith, Pico hydro for village power: A practical manual for schemes up to 5kW in hilly areas, 2001, Available from: http://www.eee.nottingham.ac.uk/picohydro/documents.html [accessed 06.27.2011]

[26] A. Williams, Pumps as turbines: a user's guide, ITDG publishing, 2003.

[27] Gilkes. The Conversion of Nature into Electricity: Gilkes Hydropower, Available from: http://www.gilkes.com/images/hydro%20general%20brochure_smaller.pdf [accessed 07.13.2011]

[28] ABS Alaskan. Hydro Power Design Booklet, Available from: http://www.absak.com/ [accessed 07.19.2011]

[29] J. Hartvigsen <joe@h-hydro.com>, Turgo Turbines, personal communication [sent 7.13.2011]

[30] ABS Alaskan, Available from: http://www.absak.com/ [accessed 07.19.2011]

[31] A. Williams, Pumps as turbines for low cost micro hydro power, J Renew Energy, 9 (1996) 1227-1234.

[32] T. Chalko, Optimizing a permanent magnet alternator for micro-hydro application, 2005, Available from: http://mtbest.net/SD_modification.pdf [accessed 08.02.2011]

[33] R.W. Fox, A.T. McDonald, P.J. Pritchard, Introduction to fluid mechanics, 6th ed., John Wiley & Sons, Hoboken, NJ, 2004.

[34] J.M. Cimbala, Y.A. Cengel, Essentials of fluid mechanics: Fundamentals and applications, McGraw-Hill, New York, 2008.

[35] P. Maher, N. Smith, The pico power pack: a new design for pico hydro, Micro Hydro Cenre, The Nottingham Trent University, 1999, Available from: http://www.eee.nottingham.ac.uk/picohydro/documents.html [accessed 06.27.2011]

[36] K. Alexander, E. Giddens, A. Fuller, Axial-flow turbines for low head microhydro systems, J Renew Energy, 34 (2009) 35-47.

[37] L. Balakrishnan, Women & micro-hydro systems, in: Himalayan Small Hydropower Summit, New Delhi, 2006.

[38] A. Zahnd, H. Kimber, R. Komp, Renewable Energy Village Power Systems for Remote and Impoverished Himalayan Villages in Nepal, in: Proc Int Conf Renew Energy for Dev Ctries, Washington, DC, 2006.

[39] M. Hallett, Distributed power in Afghanistan: The Padisaw micro-hydro project, J Renew Energy, 34 (2009) 2847-2851.

[40] N. Smith, G. Ranjitkar, Nepal Case Study - Part One: Installation and Performance of the Pico Power Pack, in: Pico Hydro, The Nottingham Trent University, Nottingham, UK, 2000, pp. 3.

[41] Practical Action, Micro-hydro Scheme, Chambamontera, Peru: Report to the Matthiesen Foundation, 2008, Available from: http://www.thematthiesenfoundation.org/docs/48285110431ec.pdf [accessed 08.02.2011]

[42] Pre-feasibility study for rural electrification program by renewable energy in the mountainous region of northern Samar in the Philippines, 2007, Available from: http://www.ecfa.or.jp/japanese/act-pf_jka/H18/renkei/wjec_philippines.pdf [accessed 06.27.2011]

[43] E. Nfah, J. Ngundam, M. Vandenbergh, J. Schmid, Simulation of off-grid generation options for remote villages in Cameroon, J Renew Energy, 33 (2008) 1064-1072.

[44] D. Singh, Renewable energy technologies in Africa–An energy training course handbook, in: S. Karekezi, W. Kithyoma, L. Majoro (Eds.), African Energy Policy Research Network, Nairobi, Kenya, 2000, pp. 54-58.

[45] E. Ilskog, 2004, And then they lived sustainably ever after? - Part I, experiences from rural electrification in Tanzania, Zambia and Kenya, Thesis for Doctor in Technology, thesis (Doctor in Technology), Luleå University of Technology

[46] A. Varghese, Small and Micro Hydro Power Related projects in Africa and Asia, 2006, Available from: http://www.unido.org/fileadmin/import/48784_Small_Hydro_Power_projects3.pdf [accessed 02.10.2011]

[47] P. Maher, Kenya case study 1: Design and implementation of a 1.1 kW pico hydro serving 65 households, Micro Hydro Cenre, The Nottingham Trent University, 2002, Available from: http://www.eee.nottingham.ac.uk/picohydro/documents.html [accessed 06.27.2011]

[48] P. Maher, Kenya case study 2: Design and implementatoin of a 2.2 kW pico hydro serving 110 households, Micro Hydro Cenre, The Nottingham Trent University, 2002, Available from: http://www.eee.nottingham.ac.uk/picohydro/documents.html [accessed 06.27.2011]

[49] J. Cherni, The sustainability of renewable energy technology for isolated rural areas: Studies in Columbia, Cuba and Peru, Available from: http://www.seeds.usp.br/pir/arquivos/congressos/CLAGTEE2003/Papers/RNCSEP%20B-248.pdf [accessed 06.27.2011]

[50] CADDET Centre for Renewable Energy, Small-scale hydro within a municipal water supply system, Technical Brochure No. 130, 2000, Available from: http://www.caddet-re.org/html/technologies.htm [accessed 08.02.2011]

[51] R. Manning, Micro projects seek to harness existing hydropower sources, 2010, Available from: http://news.opb.org/article/17777-micro-projects-seek-harness-existing-hydropower-sources/ [accessed 06.27.2011]

[52] B. Eaton, J. Mitchell, H. Harding, Porirua low-level reservoir - mini-hydro feasibility study, 2009, Available from: http://www.eeca.govt.nz/node/10909 [accessed 08.02.2011]

[53] H.J.R. Driscoll, Micro-hydro power in Dorset: A re-assessment of potential installed capacity, in: Earth & E-nvironment, University of Leeds Press, W. Yorkshire, IK, 2007-08, pp. 52-114.

[54] J. Reeger, Water plant goes with flow to reduce electricity costs, October 2, 2010, Available from: http://www.pittsburghlive.com/x/pittsburghtrib/news/westmoreland/s_702414.html [accessed 06.27.2011]

[55] Highland Eco-Design, Micro-hydro in scotland: How can I use it?, Available from: http://www.cifalfindhorn.org/docs/HighHead_SiteSelection_Syst.pdf [accessed 06.27.2011]

[56] W. Klunne, The low head microhydro at Derendingen in Switzerland, Available from: http://envirostewards.rutgers.edu/Lecture%20Resource%20Pages/Energy%20resources/Small%20Hydro/%5Bmicrohydropower_net%5D%20Derendingen%20case%20study.htm [accessed 06.27.2011]

[57] L. Richardson, Rhyd Hall Microhydro Feasibility Study, 2008, Available from: http://www.scienceshopswales.org.uk/documents/Completed%20Reports/33.03_LR_Rhyd%20Hall%20Microhydro%20Feasibility%20Study.pdf [accessed 06.27.2011]

[58] E. White, S. Davis, P. Grange, J. Booth, Microhydro feasibility study for salt spring island, 2009, Available from: http://www.saltspringenergystrategy.org/docs/Microhydro.pdf [accessed 08.02.2011]

[59] T. Goodman, Feasibility study report, Te Mapoupa Papakainga Trust and The Energy Efficiency and Conservation Authority, 2010, Available from: http://www.eeca.govt.nz/sites/all/files/dg-fund-maungapohatu-oct-2010.pdf [accessed 08.02.2011]

[60] T. Bailey, R. Bass, Hydroelectric feasibility study: An assessment of the feasibility of generating electrical power using urban stormwater in Oregon City, 2009, Available from: http://www.oit.edu/libraries/portland_osp/oc_hydro_study_report_r1.pdf [accessed 06.27.2011]

[61] M. Matlock, K. Kersey, C. Riding In, Pawnee Nation of Oklahoma Energy Options Analysis, 2009, Available from: http://apps1.eere.energy.gov/tribalenergy/pdfs/pawnee_final_report.pdf [accessed 08.02.2011]

[62] C. Miller, Hoopa Valley Small Scale Hydroelectric Feasibility Project, Hoopa Valley Tribal Council, 2009, Available from: http://apps1.eere.energy.gov/tribalenergy/pdfs/hoopa_valley_final%20report.pdf [accessed 08.02.2011]

[63] M. Tamburrini, 2004, A Feasibility Study for a Micro-hydro Installation for the Strangford Lough Wildfowlers & Conservation Association, thesis, University of Strathclyde, Glasgow, UK

[64] The Haven Trust, Waione Falls Micro Hydro Project Feasibility Report, 2010, Available from: http://www.eeca.govt.nz/sites/all/files/dg-fund-waione-falls-oct-2010.pdf [accessed 06.27.2011]

[65] S. Derakhshan, A. Nourbakhsh, Experimental study of characteristic curves of centrifugal pumps working as turbines in different specific speeds, J Exp Therm Fluid Sci, 32 (2008) 800-807.

[66] J. Kenfack, F.P. Neirac, T.T. Tatietse, D. Mayer, M. Fogue, A. Lejeune, Microhydro-PV-hybrid system: Sizing a small hydro-PV-hybrid system for rural electrification in developing countries, J Renew Energy, 34 (2009) 2259-2263.

[67] E. Nfah, J. Ngundam, Feasibility of pico-hydro and photovoltaic hybrid power systems for remote villages in Cameroon, J Renew Energy, 34 (2009) 1445-1450.

[68] S. Ashok, Optimised model for community-based hybrid energy system, J Renew Energy, 32 (2007) 1155-1164.

[69] Homer Energy, Available from: http://www.homerenergy.com/ [accessed 06.24.2011]

[70] K. Alexander, E. Giddens, A. Fuller, Radial-and mixed-flow turbines for low head microhydro systems, J Renew Energy, 34 (2009) 1885-1894.

[71] R. Simpson, A. Williams, Application of computational fluid dynamics to the design of pico propeller turbines, in: Proc Renew Energy Dev Ctries, Washinton, DC, April 7, 2006.

[72] J.S. Anagnostopoulos, D.E. Papantonis, Flow modeling and runner design optimization in turgo water turbines, Int J Appl Sci, Eng and Technol, (2007) 6.

[73] J. Razak, Y. Ali, M. Alghoul, M.S. Zainol, A. Zaharim, K. Sopian, Application of crossflow turbine in off-grid pico hydro renewable energy system, in, World Scientific and Engineering Academy and Society (WSEAS), 2010, pp. 519-526.

[74] B. Zoppé, C. Pellone, T. Maitre, P. Leroy, Flow analysis inside a Pelton turbine bucket, J Turbomach, 128 (2006) 500.

[75] K. Patel, B. Patel, M. Yadav, T. Foggia, Development of Pelton turbine using numerical simulation, IOP conference series: Earth and environmental science, 12 (2010).

[76] A. Santolin, G. Cavazzini, G. Ardizzon, G. Pavesi, Numerical investigation of the interaction between jet and bucket in a Pelton turbine, in: Proc IMechE J Power Energy, 2009, pp. 721-728.

[77] M. Peron, E. Parkinson, L. Geppert, T. Staubli, Importance of jet quality on Pelton efficiency and cavitation, in: IGHEM 2008, Milan, Italy, September 3-6, 2008.

[78] B. Singh, S. Murthy, S. Gupta, An electronic voltage and frequency controller for single-phase self-excited induction generators for pico hydro applications, in: Proc Power Elec Drives Sys, IEEE, Kuala Lumpur, Malaysia, November 28-December 1, 2005, pp. 240-245.

[79] M.G. Molina, M. Pacas, Improved power conditioning system of micro-hydro power plant for distributed generation applications, Int Conf on Ind Technol, (March 14-17, 2010) 1733-1738.

[80] I. Salhi, S. Doubabi, Fuzzy controller for frequency regulation and water energy save on micro-hydro electrical power plants, in: International renewable energy congress, Sousse, Tunisia, November 5-7, 2009, pp. 106-112.

[81] D. Howey, Axial flux permanent magnet generators for pico-hydropower, in: EWB-UK Research Conference, Royal Academy of Engineers, 2009, pp. 8.

[82] S. Dunnett, H. Piggott, Axial airgap machines for small wind generators in developing countries, in: IEE Conference Digest, 2001.

[83] D. Agar, M. Rasi, On the use of a laboratory-scale Pelton wheel water turbine in renewable energy education, J Renew Energy, 33 (2008) 1517-1522.

[84] J. Baines, A. Williams, A test rig for pico hydro Pelton turbines, in: Pico Hydro News, The Nottingham Trent University, Nottingham, UK, 1997, pp. 7-8.

[85] P. Singh, F. Nestmann, Experimental optimization of a free vortex propeller runner for micro hydro application, Exp Therm Fluid Sci, 33 (2009) 991-1002.

[86] P. Gautam, B. Thapa, The KU's water power laboratory, Available from: http://www.ku.edu.np/mech/water_power_laboratory/Kathmandu_University_Water_Power_Laboratory.htm [accessed 06.27.2011]

[87] A. Wheeler, Introduction to engineering experimentation, 2nd ed., Prentice Hall, Upper Saddle River NJ:, 2003.

[88] D. Halliday, R. Resnick, J. Walker, Fundamentals of physics, 6th ed., John Wiley & Sons, New York, 2001.

[89] T. Sebastian, Temperature effects on torque production and efficiency of PM motors using NdFeB magnets, IEEE Trans Ind Appli, 31 (1995) 353-357.

[90] Industrial pumps catalog, series 30 60 80 110, Available from: http://www.mppumps.com/non-html/catalog/industrial/catalog_ind_series.pdf [accessed 06.23.2011]

APPENDICES

Appendix A – Pump Performance Curve

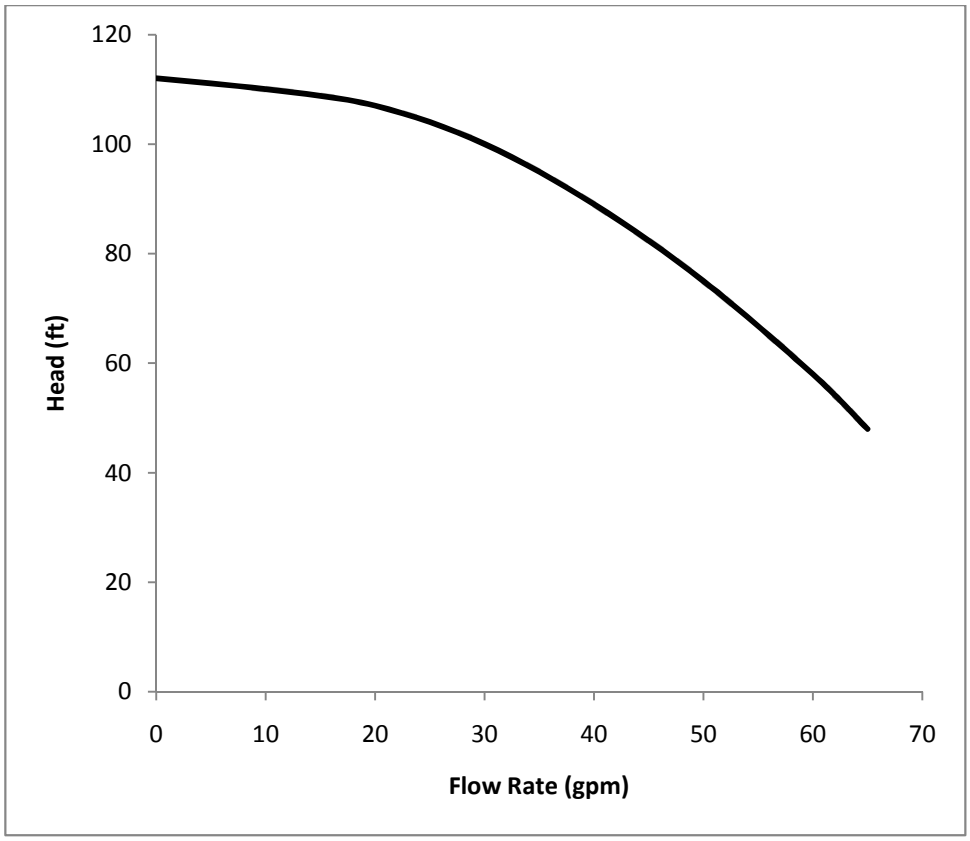

Fig. A.1. Pump performance curve for Series 60 centrifugal pump (MP Pumps, Frazier, MI, adapted from [90]).

Appendix B: Sample Datasheets

B.1 Turbine Datasheet

Turbine Specs (Type, PCD):

Test Condition

Nozzle Size (in)	
Jet Angle (°)	
Radius (in)	
Elevation (in)	
Distance (in)	

	Data Point											
Test Condition	Parameter	1	2	3	4	5	6	7	8	9	10	11
A	Pressure (psi)											
	Flow Rate (gpm)											
	Temperature (°C)											
	Speed (RPM)											
	Force (lb, oz)											
B	Pressure (psi)											
	Flow Rate (gpm)											
	Temperature (°C)											
	Speed (RPM)											
	Force (lb, oz)											
C	Pressure (psi)											
	Flow Rate (gpm)											
	Temperature (°C)											
	Speed (RPM)											
	Force (lb, oz)											
D	Pressure (psi)											
	Flow Rate (gpm)											
	Temperature (°C)											
	Speed (RPM)											
	Force (lb, oz)											

Fig. B.1. Sample datasheet used for turbine testing.

B.2 Generator Datasheet

N (RPM)	Force	Voltage	Current
600			
700			
800			
900			
1000			
1100			
1200			
1300			

N (RPM)	Force	Voltage	Current
1400			
1500			
1600			
1700			
1800			
1900			
2000			

Fig. B.1. Sample datasheet used for generator testing.